

---


Electronic Theses and Dissertations, 2004-2019

---

2013

## Similarity Of Climate Control On Base Flow And Perennial Stream Density In The Budyko Framework

Liuliu Wu  
*University of Central Florida*

 Part of the [Engineering Commons](#), and the [Water Resource Management Commons](#)  
Find similar works at: <https://stars.library.ucf.edu/etd>  
University of Central Florida Libraries <http://library.ucf.edu>

This Masters Thesis (Open Access) is brought to you for free and open access by STARS. It has been accepted for inclusion in Electronic Theses and Dissertations, 2004-2019 by an authorized administrator of STARS. For more information, please contact [STARS@ucf.edu](mailto:STARS@ucf.edu).

---

### STARS Citation

Wu, Liuliu, "Similarity Of Climate Control On Base Flow And Perennial Stream Density In The Budyko Framework" (2013). *Electronic Theses and Dissertations, 2004-2019*. 2824.  
<https://stars.library.ucf.edu/etd/2824>

SIMILARITY OF CLIMATE CONTROL ON BASE FLOW AND PERENNIAL STREAM  
DENSITY IN THE BUDYKO FRAMEWORK

by

LIULIU WU  
B.S. Hohai University, 2009  
M.S. Hohai Univeristy, 2011

A thesis submitted in partial fulfillment of the requirements  
for the degree of Master of Science  
in the Department of Civil, Environmental, and Construction Engineering  
in the College of Engineering and Computer Sciences  
at the University of Central Florida  
Orlando, Florida

Spring Term  
2013

Major Professor: Dingbao Wang

© 2013 Liuliu Wu

## ABSTRACT

Streams are classified into perennial, intermittent, and ephemeral streams based on flow durations. Perennial stream is the basic network, while intermittent or ephemeral stream is the expanded network. Connection between perennial stream and base flow at the mean annual scale exists since one of the hydrologic functions of perennial stream is to deliver runoff even in low flow seasons. The partitioning of precipitation into runoff and evaporation at the mean annual scale, on the first order, is captured by the ratio of potential evaporation to precipitation ( $E_p/P$  called climate aridity index) based on the Budyko hypothesis.

The primary focus of this thesis is the relationship between base flow and perennial stream density ( $D_p$ ) in the Budyko framework. In this thesis, perennial stream density is quantified from the high resolution National Hydrography Dataset for 185 watersheds; the climate control (represented by the climate aridity index) on perennial stream density and on base flow is quantified; and the correlation between base flow and perennial stream density is analyzed.

Perennial stream density declines monotonically with the climate aridity index, and an inversely proportional function is proposed to model the relationship between  $D_p$  and  $E_p/P$ . This monotonic trend of perennial stream density reconciles with the Abrahams curve, and the perennial stream density is only a small portion of the total drainage density. The dependences of base flow ratio ( $Q_b/P$ ) and the normalized perennial stream density on the climate aridity index follow a similar complementary Budyko-type curve. The correlation coefficient between

the ratio of base flow to precipitation and perennial stream density is found to be 0.74. The similarity between the base flow and perennial stream density reveals the co-evolution between water balance and perennial stream network.

I dedicate this thesis to loved people.

## ACKNOWLEDGMENTS

I would first and foremost like to thank my academic advisor Dr. Dingbao Wang, without him, I would not have had the opportunity to complete this research. He has been an extraordinary advisor. He teaches me how to be a researcher. I will always remember his telling me to be creativity on thinking. His continued guidance, support, and ideas have allowed me to fully recognize my potential as a researcher. I would like to thank my committee members Dr. Manoj Chopra and Dr. David M. Sumner, who offered intellectual support and academic guidance.

I am truly thankful for the love and support of my family. My dearest father and mother, Zhenjiang and Meiliang, they do the hardest decision to let me leave them to pursue my dream to a very far away country for a long time. Without their self-sacrifice, encourage and sound advice throughout my study at UCF, I never would have gotten to this point. I am so proud to be your children. I must send my love and well wishes to my lovely brother, Huolian, for his continuous unconditional support and believe in me not only in normal life but also in academy study.

I would also like to thank my friends who have greatly impacted my time at UCF: Sihui He, Xiang Ji, Ganesh, Xi Chen, Murat, Stephaney, Andrew, and Nader. Without your support, guidance and share I would have not enjoyed graduate life in Orlando. Special thanks to Sihui He, Xiang Ji and Ganesh. Without you guys, I do believe I cannot go on anymore.

Last but not least, I would like to thank my everlasting friends, Chaoqun Liu, Xiaobin Wang, Yin Liao, Jiandong, Zhen Li, and Hongtao Zhao, who although are far away from me, but I received their support, friendship and love very day.



# TABLE OF CONTENTS

LIST OF FIGURES .....	x
LIST OF TABLES .....	xii
CHAPTER 1: INTRODUCTION .....	1
1.1 Water Balance .....	1
1.2 Drainage Density and Perennial Stream .....	1
1.3 Background .....	2
1.4 Objectives .....	3
1.5 Organization of the Thesis .....	3
CHAPTER 2: LITERATURE REVIEW .....	5
2.1 Stream Classification .....	5
2.2 Drainage Density .....	7
2.3 Water Balance .....	8
CHAPTER 3: METHODOLOGY .....	9
3.1 Data Sources .....	9
3.1.1 International Model Parameter Estimation Experiment .....	9
3.1.2 National Hydrography Dataset .....	15

3.1.3 Base Flow.....	19
3.2 Budyko Framework .....	21
3.3 Perennial Stream Density as a Function of Climate Aridity Index.....	24
CHAPTER 4: RESULTS AND DISCUSSIONS .....	25
4.1 Results.....	25
4.2 Discussions .....	32
4.2.1 Perennial, Intermittent, Ephemeral, and Total Stream Densities.....	32
4.2.2 Normalized Perennial Stream Density.....	37
4.2.3 Impact of Slope on Perennial Stream Density .....	38
4.2.4 Application of the Relationship between Perennial Stream Density and Climate Aridity Index.....	39
CHAPTER 5: CONCLUSIONS AND RECOMMENDATIONS .....	41
REFERENCES .....	42

## LIST OF FIGURES

Figure 3.1. Spatial distribution of drainage areas for the 185 study watersheds. ....	10
Figure 3.2. The histogram of drainage areas for the 185 study watersheds.....	10
Figure 3.3. Spatial distribution of mean annual precipitation ( $P$ ) for the 185 study watersheds..	11
Figure 3.4. The histogram of mean annual precipitation ( $P$ ) for the 185 study watersheds. ....	11
Figure 3.5. Spatial distribution of mean annual runoff ( $Q$ ) for the 185 study watersheds. ....	12
Figure 3.6. The histogram of mean annual runoff ( $Q$ ) for the 185 study watersheds.....	12
Figure 3.7. Spatial distribution of climate aridity index ( $E_p/P$ ) for the 185 study watersheds. ....	13
Figure 3.8. The histogram of climate aridity index ( $E_p/P$ ) for the 185 study watersheds. ....	13
Figure 3.9. The mean annual precipitation ( $P$ ) and the mean annual runoff ( $Q$ ) for the 185 study watersheds.....	15
Figure 3.10. Spatial distribution of perennial stream length ( $L_p$ ) for the 185 study watersheds. .	18
Figure 3.11. The histogram of perennial stream length ( $L_p$ ) for the 185 study watersheds.....	19
Figure 3.12. The base flow separation result for Snoqualmie River watershed, Washington with USGS gage 12149000 during January 1 <sup>th</sup> , 1960 to March 1 <sup>th</sup> , 1960.....	20
Figure 3.13. Comparison of observed evaporation ratio ( $E/P$ ) with estimates based on Budyko curve at the 185 study watersheds. ....	22
Figure 3.14. $Q_b/P$ versus $E_p/P$ , and the fitted complementary Turc-Pike curve.....	23

Figure 4.1. Temporal stream and perennial stream: a) Snoqualmie River watershed, Washington with USGS gage 12149000,  $E_p/P=0.29$ ,  $D_p=1.60 \text{ km}^{-1}$ ; b) Red Creek watershed, Mississippi with USGS gage 02479300,  $E_p/P=0.70$ ,  $D_p=0.48 \text{ km}^{-1}$ ; c) Elm Fork Trinity River watershed, Texas with USGS gage 08055500,  $E_p/P=1.77$ ,  $D_p=0.27 \text{ km}^{-1}$ ; d) Arroyo Chico watershed, New Mexico with USGS gage 08340500,  $E_p/P=5.50$ ,  $D_p=0.067 \text{ km}^{-1}$ . ..... 27

Figure 4.2. Spatial distribution of perennial stream densities ( $D_p$ ) for the 185 study watersheds. .... 28

Figure 4.3. The histogram of perennial stream densities ( $D_p$ ) for the 185 study watersheds. .... 29

Figure 4.4. NHD-based perennial stream density,  $D_p$  ( $\text{km}^{-1}$ ), and the fitted line are plotted as a function of climate aridity index ( $E_p/P$ )..... 31

Figure 4.5. The correlation coefficient between perennial stream density ( $D_p$ ) and base flow coefficient ( $Q_b/P$ ) is 0.74. .... 32

Figure 4.6. Total drainage density (*Abraham*, 1984) and perennial stream density as a function of *PE* index..... 33

Figure 4.7. The correlation between *PE* index and climate aridity index ( $E_p/P$ ) for the 160 study watersheds with *PE* index less than 500. .... 34

Figure 4.8. Perennial, intermittent and ephemeral streams and runoff generation from mean annual to seasonal and to event scales. .... 36

Figure 4.9.  $D_p/D_p^*$  versus  $E_p/P$  and the fitted complementary Turc-Pike curve for  $Q_b/P$  versus  $E_p/P$ . .... 38

Figure 4.10. Perennial stream density versus slope (%) for the 185 study watersheds. .... 39

**LIST OF TABLES**

Table 3.1. The types of flow lines (Fcodes) contained in perennial stream length calculation in NHD..... 17

# CHAPTER 1: INTRODUCTION

## 1.1 Water Balance

The water moves on, above and below the surface of the earth is known as the water cycle, also called as the hydrologic cycle. Cooler temperature causes water vapor to condense into precipitation, which falls onto the land. A portion of the water flows over the land surface as surface runoff; a portion infiltrates into the soil and further percolates into the groundwater. A portion of the water flows back to the atmosphere by evaporation. Water balance at the watershed scale has been well studied. Although the water balance remains fairly constant over time at the global scale, the water balance varies at various temporal scales.

Runoff includes both surface runoff and groundwater discharge into rivers. Base flow is the portion of runoff that comes from shallow groundwater storage. Base flow is also called slow flow since its residence time is longer than that of surface runoff.

## 1.2 Drainage Density and Perennial Stream

Drainage density is the length of the stream channel per unit area of drainage basin, which can be calculated by the total length of all the streams in a drainage basin divided by the total area of the drainage basin. It is a balance between the erosive power of surface runoff and the resistance of surface soils and rocks (*Bhagwat, 2009*). Therefore, drainage density depends upon both climate and physical characteristics of the drainage basin, including topography, soil

infiltration capacity, vegetation and geology. Drainage density provides a useful numerical measure on how well or poorly a watershed is drained by stream channels both from geomorphology and hydrology (*Ritter, 2006*). Perennial stream density is the ratio between the total perennial stream length and the drainage area. Perennial stream density is only a small portion of the total drainage density (*Wang and Wu, 2013*).

From the perspective of flow duration, streams are categorized into perennial, intermittent, and ephemeral streams. Perennial stream, i.e., the basic stream network, flows for much of the year is governed by groundwater flow and therefore depends upon mean annual precipitation as modified by watershed characteristics. A temporal stream, including intermittent and ephemeral streams, occurs once or more each year and is a response to seasonal climate and individual rainfall event (*Gregory, 1976*).

### **1.3 Background**

The basic functions of a watershed include partition of collected water into different flow paths, storage of water in different parts of the watershed, and release of water from the watershed (*Wagner, et al., 2007*). Delivering the runoff generated in a watershed is one of the major hydrologic functions of stream network. On this basis, stream densities can be related to runoff in a watershed.

*Budyko (1958)* postulated that mean annual evaporation from a watershed could be determined, to first order, from precipitation and potential evaporation. Based on world-wide data on a large number of watersheds, *Budyko (1974)* demonstrated that the partitioning of

precipitation into runoff and evaporation is primarily controlled by the climate aridity index. Perennial stream density may be dependent on both mean annual precipitation and potential evaporation similar to mean annual runoff, particularly base flow.

#### **1.4 Objectives**

The followings are specific research objectives of this study:

- I. Examine the dependences of base flow on climate aridity index in the Budyko framework.
- II. Quantify the dependences of perennial stream density on climate aridity index in the Budyko framework.
- III. Explore the co-evolution of water balance and perennial streams.
- IV. Compare the findings on perennial stream with the Abrahams curve (*Abrahams, 1984*) on the total drainage density.
- V. Discuss the linkage between runoff from the mean annual to event scales and perennial, intermittent and ephemeral stream densities.

#### **1.5 Organization of the Thesis**

The thesis includes 4 Chapters to represent the concepts of the indicated research tasks.

- Chapter 1: Introduction – This chapter introduces water cycle, drainage density, perennial stream and some other basic concepts which are studied in this thesis research. It also



contains some background information which motivated this research, and overall objectives defined and accomplished in this research.

- Chapter 2: Literature review – The literature on stream classifications, drainage density, and water balance is summarized and reviewed. This chapter provides theoretical supports and background for the goal of this research.
- Chapter 3: Methodology – Information about the data sources is presented, including the drainage area, mean annual precipitation, mean annual runoff, climate aridity index, and perennial stream length for the 185 study watersheds. The Budyko framework and the climate aridity index is discussed. The method applied in this research to identify perennial stream density as a function of climate aridity index is described.
- Chapter 4: Results and discussions – This chapter shows the results of this research. The relationships between perennial, intermittent, ephemeral and total stream densities are presented. The normalized perennial stream density is discussed. The impact of slope on perennial stream density is briefly explored. The application of the relationship between perennial stream density and the climate aridity index is discussed.
- Chapter 5: Conclusions and recommendations – The findings of this research are summarized and the further potential research is recommended.

## CHAPTER 2: LITERATURE REVIEW

### 2.1 Stream Classification

In a watershed, the flowing stream network expands to respond rainfall events and contracts during drought periods (*Blyth and Rodda, 1973; Gregory, 1976; Day, 1978*). Stream classification definitions vary but most often from the perspective of flow duration, streams are categorized into perennial, intermittent, and ephemeral streams. Perennial stream, i.e., the basic stream network, flows for much of the year is governed by groundwater flow and therefore depends upon mean annual precipitation as modified by watershed characteristics; the temporal streams, i.e., intermittent and ephemeral streams, occurs once or more each year and is a response to seasonal climate and individual rainfall event (*Gregory, 1976*).

The differentiation between perennial and temporal streams is not quantitatively definite, and subject to a variety of definitions adopted by regulation agencies and academics with a need to classify streamflow durations. Therefore, definitions of perennial and temporal streams vary widely among regulatory agencies.

The federal regulation defining perennial stream “means a stream or part of a stream that flows continuously during all of the calendar year as a result of ground-water discharge or surface runoff”. Ephemeral streams means streams that flow only when it rains and intermittent streams are those streams do not flow continuously at least seasonally. Kentucky Forestry BMP guidelines define “perennial stream: streams that hold water throughout the year. Intermittent: streams that hold water during wet portions of the year. Ephemeral: a channel formed by water

during or immediately after precipitation events” (*Stringer and Perkins, 2001*). Some states quantitatively determine stream class. For example, Texas classify the stream under normal climatic conditions as perennial streams when it flows greater than 90% of the year, as ephemeral streams when it flows less than 30% of the year, and seasonal flows between these two thresholds are considered as intermittent streams (*Texas Forest Service, 2000*).

The several methods are applied in academics. *Hewlett (1982) and Svec et al., (2005)* used the same threshold 90% for determine the perennial stream. *Hedman and Ostekamp (1982)* used the threshold 80% and 10% percent of the time of the measurable surface discharge to defined perennial streams. A perennial stream is defined as a river channel that has continuous flow on the stream bed all year round during years of normal rainfall (*Meinzer, 1923*). Whether connect to base flow or water table is another kind of method to classify stream. *Paybin (2003)* considered a stream as perennial stream when base flow contribute it year round, while as ephemeral channel if it does not receive base flow at any time of year. As base-flow contributions to the channel seasonally, it is defined as intermittent stream. Perennial streams are defined as having 7-day, 10-year low flows greater than zero by *Hunrichs (1983)*. During unusually dry years, a normally perennial stream may cease flowing, becoming intermittent for days, weeks, or months depending on severity of the drought (*Ivkovic, 2009*). Perennial stream in the NHD dataset is defined as “stream contains water throughout the year, except for infrequent periods of severe drought” (*Simley, 2006*).

## 2.2 Drainage Density

Total drainage density, defined as the total length of channels per unit area (*Horton*, 1932; *Horton*, 1945), is known to vary with climate and vegetation (*Melton*, 1957), soil and rock properties (*Carlston*, 1963; *Kelson and Wells*, 1989), and topography (*Montgomery and Dietrich*, 1988). *Melton* (1957) explored the dependence of drainage density on the *Thornthwaite's* (1931) precipitation effectiveness index (i.e., *PE* index) which is a measure of the availability of moisture to vegetation, and found a negative correlation between drainage density and *PE* index. *Madduma Bandara* (1974) extended the samples to cover watersheds in the humid Sri Lanka and a positive correlation was found between drainage density and *PE* index. Therefore, drainage density decreases but then increases from arid to humid regions (*Abrahams*, 1984), and this trend has been explained by the vegetation imparted to the soil (e.g., *Moglen et al.*, 1998) and demonstrated in landscape evolution models (e.g., *Perron et al.*, 2007; *Collins and Bras*, 2010).

*De Wit and Stankiewicz* (2006) studied the relation between perennial stream density ( $D_p$ ) and mean annual precipitation in Africa. They found that  $D_p$  is close to zero when precipitation is less than 400 mm/year; from 400 mm/year to 1000 mm/year,  $D_p$  increases with precipitation and then decreases when precipitation is larger than 1000 mm/year. The linkage between drainage density and frequency regimes of peak flows has also been discussed in the literature (*Merz and Blöschl*, 2008; *Pallard, et al.*, 2009).

Interactions between climate, soil, vegetation, and topography contribute to the generation of observed patterns in natural watersheds, and the patterns contain valuable information about the way they function (*Sivapalan*, 2005). The dependence of perennial stream

density on mean climate deserves further investigation for assessing potential climate change impact on water supply availability.

### **2.3 Water Balance**

Functional patterns offer an insight on the mechanisms and processes driving the observed natural structure (*Sivapalan et al.*, 2011). The functional approach may provide answers as to why streams and their associated densities organize the way they do. The basic functions of a watershed include partition of collected water into different flowpaths, storage of water in different parts of the watershed, and release of water from the watershed (*Wagner, et al.*, 2007). Delivering the runoff generated in a watershed is one of the major hydrologic functions of stream network. On this basis, stream densities can be related to runoff in a watershed. *Berger and Entekhabi* (2001) and *Sankarasubramanian and Vogel* (2002b) studied the correlations between runoff coefficient and physiographic and climate variables (i.e., climate aridity index, drainage density, median slope, relief ratio, infiltration capacity), and found that the ratio of potential evaporation and precipitation ( $E_p/P$ ), which is called climate aridity index, explains most of variability of observed runoff coefficient which is also correlated with drainage density.

However, runoff at the mean annual scale is not only controlled by water supply but also energy supply. *Budyko* (1958) postulated that mean annual evaporation from a watershed could be determined, to first order, from precipitation and potential evaporation. Based on world-wide data on a large number of watersheds, *Budyko* (1974) demonstrated that the partitioning of precipitation into runoff and evaporation is primarily controlled by climate aridity index.

## CHAPTER 3: METHODOLOGY

### 3.1 Data Sources

#### 3.1.1 International Model Parameter Estimation Experiment

The international Model Parameter Estimation Experiment (MOPEX) watersheds are chosen as case study watersheds because precipitation, potential evaporation and runoff datasets are available. The MOPEX dataset is described by *Duan et al.* (2006). This dataset includes daily values of areal precipitation, climatologic potential evaporation, and streamflow with an adequate number of precipitation gauges. Several recent studies have been based on the MOPEX watersheds (e.g., *Sivapalan et al.*, 2011; *Harman et al.*, 2011; *Wang and Hejazi*, 2011; *Wang and Alimohammadi*, 2012; *Wang and Wu*, 2013). Due to the missing data in MOPEX, 185 watersheds are selected in this study. Figure 3.1 to figure 3.8 provides special distribution and histogram of the area, mean annual precipitation, mean annual runoff and climate aridity index of the 185 study watersheds.

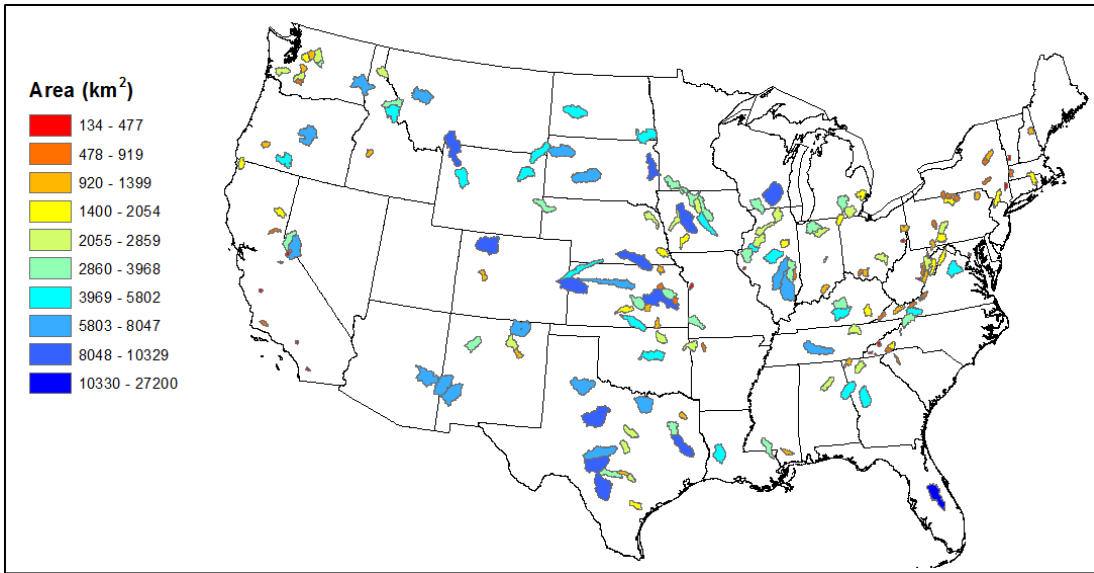


Figure 3.1. Spatial distribution of drainage areas for the 185 study watersheds.

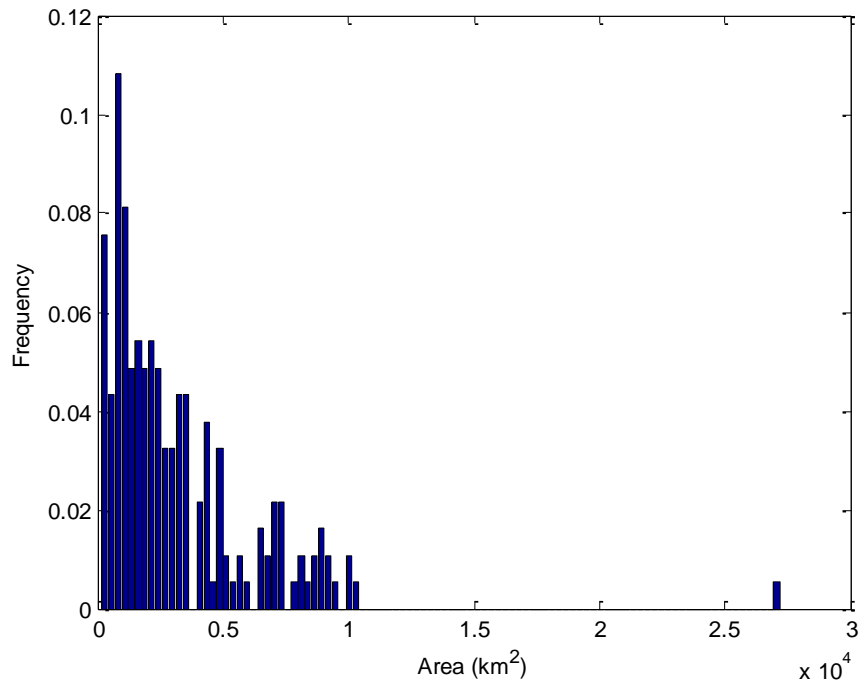


Figure 3.2. The histogram of drainage areas for the 185 study watersheds.

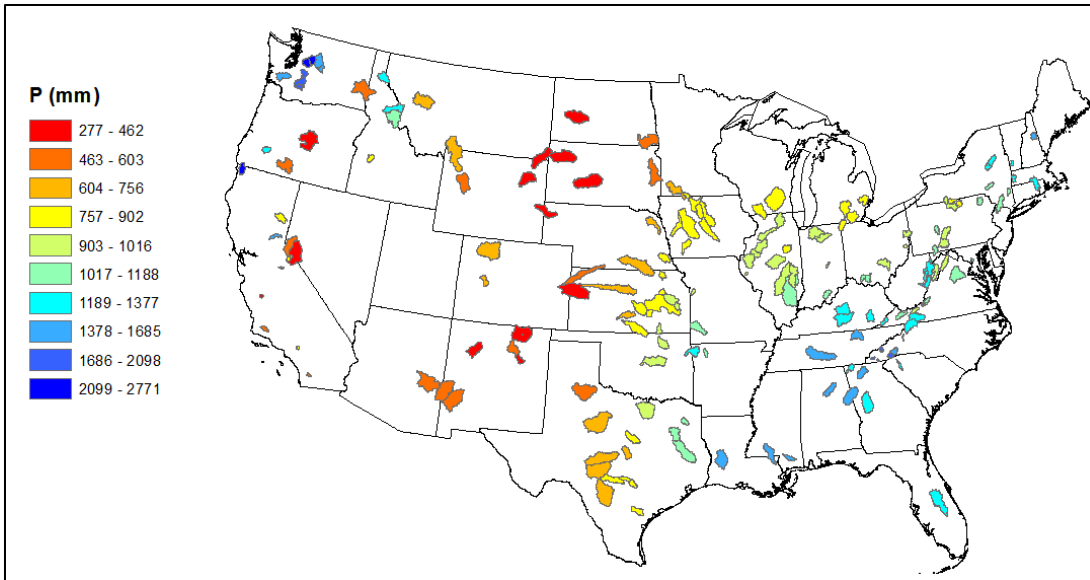


Figure 3.3. Spatial distribution of mean annual precipitation ( $P$ ) for the 185 study watersheds.

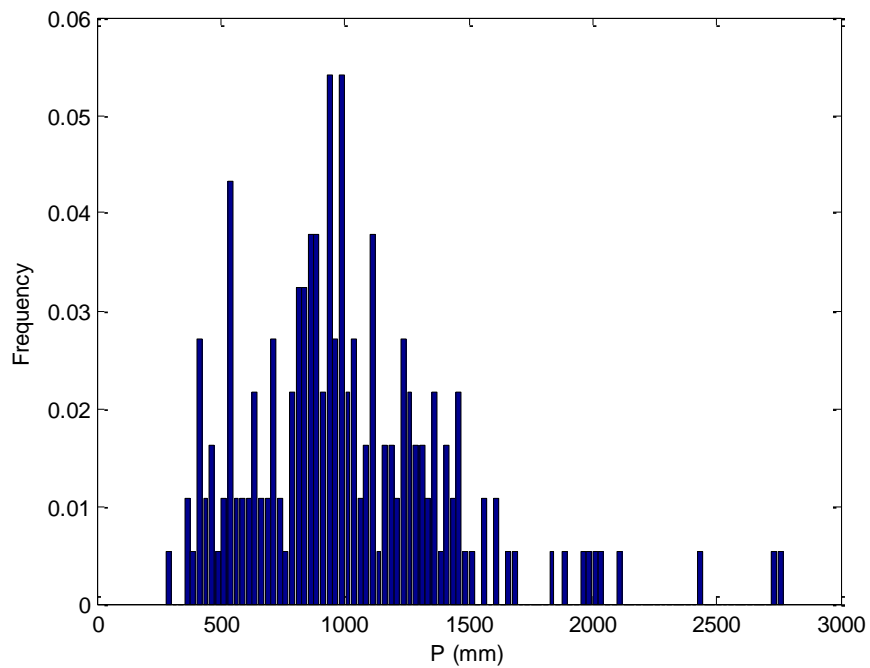


Figure 3.4. The histogram of mean annual precipitation ( $P$ ) for the 185 study watersheds.



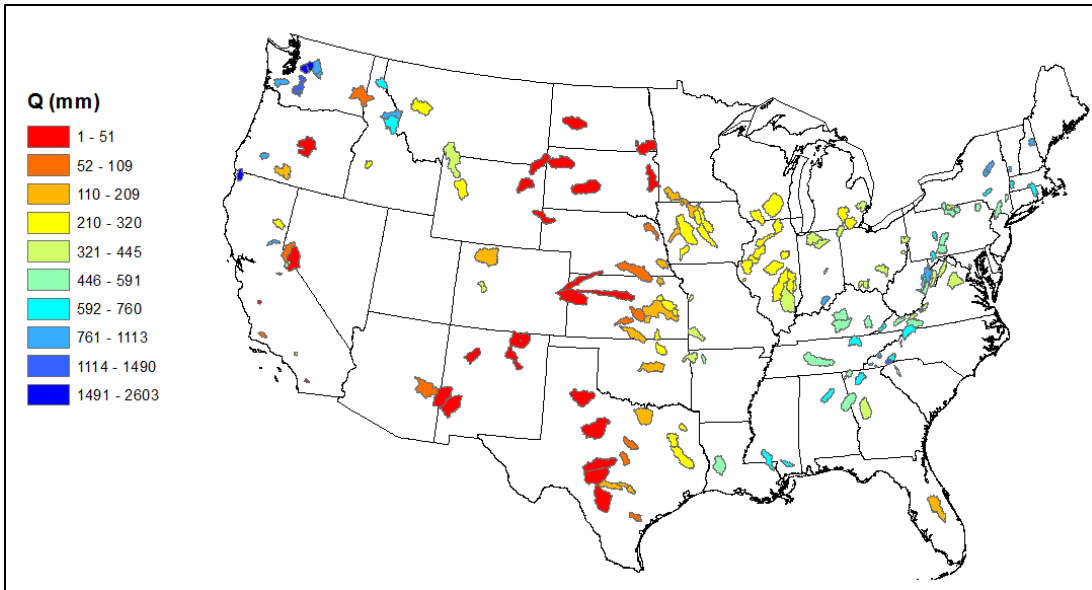


Figure 3.5. Spatial distribution of mean annual runoff ( $Q$ ) for the 185 study watersheds.

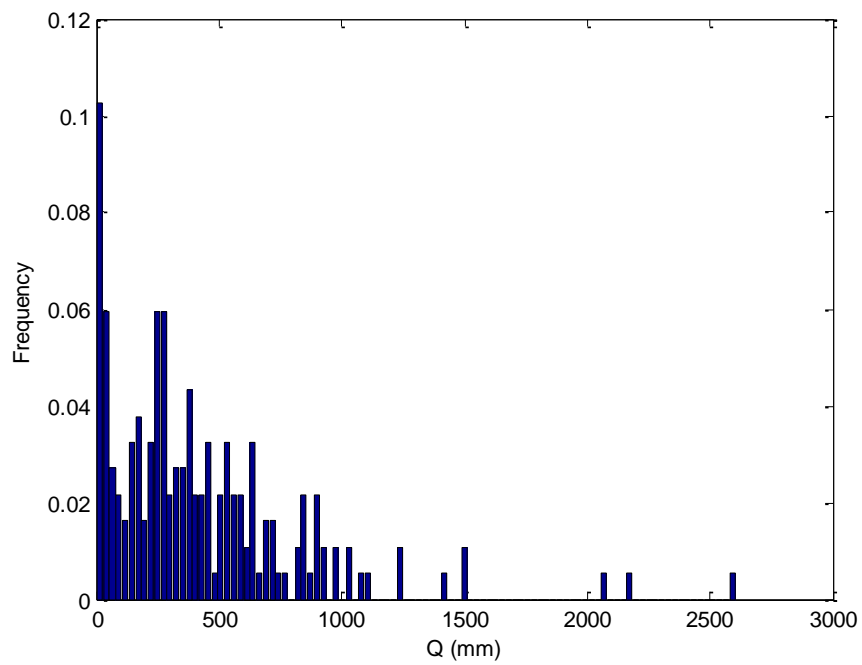


Figure 3.6. The histogram of mean annual runoff ( $Q$ ) for the 185 study watersheds.

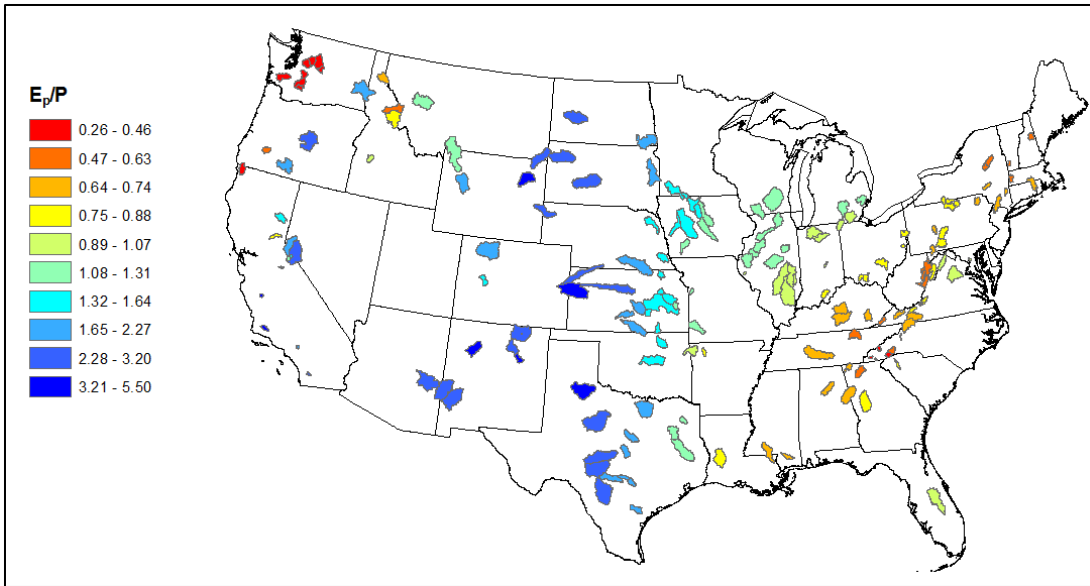


Figure 3.7. Spatial distribution of climate aridity index ( $E_p/P$ ) for the 185 study watersheds.

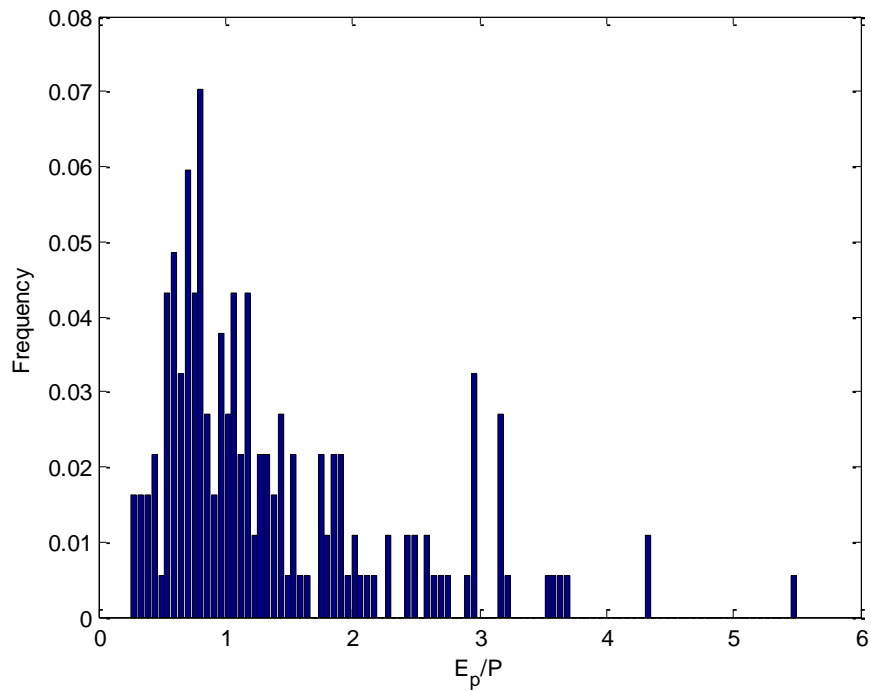


Figure 3.8. The histogram of climate aridity index ( $E_p/P$ ) for the 185 study watersheds.

Over the study watersheds, the drainage area ranges from 134 km<sup>2</sup> to 27200 km<sup>2</sup>. Most of the study watersheds are around the drainage area of 2000 km<sup>2</sup>. The High Plains has relatively lower mean annual precipitation and mean annual runoff, and higher climate aridity index, compared with eastern U.S.

The minimum mean annual precipitation is 277 mm, and the maximum mean annual precipitation is 2771 mm. While the minimum mean annual runoff is 1 mm, and the maximum mean annual runoff is 2603 mm for the 185 study watersheds. Most of the study watersheds have the mean annual precipitation ranging from 500 mm to 1500 mm. The mean annual runoff is less than 1000 mm. The climate aridity index ranges from 0.26 (humid) to 5.50 (arid). The study watersheds cover a large range of the climate aridity indexes.

Figure 3.9 shows a strong correlation between the mean annual precipitation and the mean annual runoff.

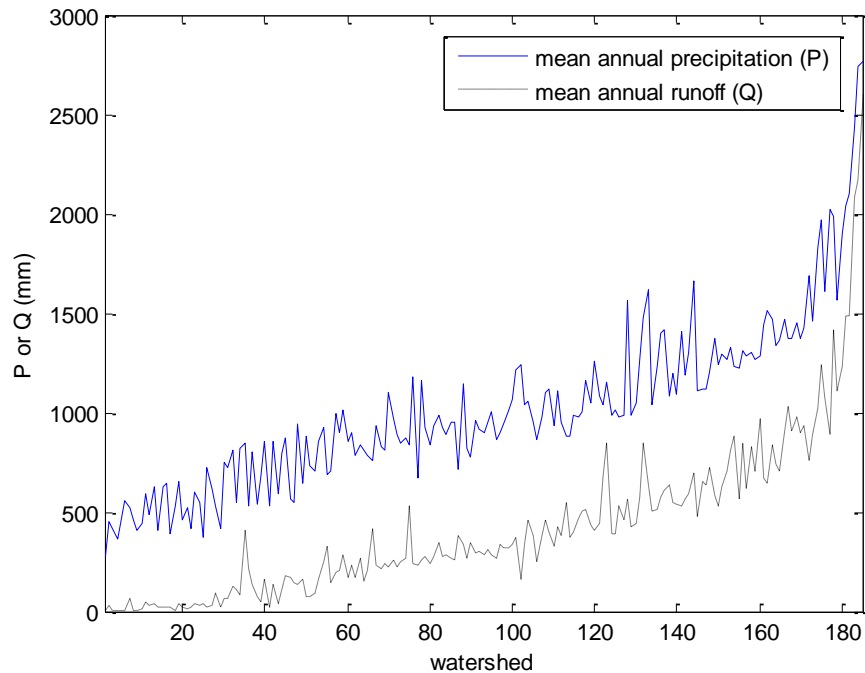


Figure 3.9. The mean annual precipitation ( $P$ ) and the mean annual runoff ( $Q$ ) for the 185 study watersheds.

### 3.1.2 National Hydrography Dataset

Perennial streams are obtained from the National Hydrography Dataset (NHD) which is a comprehensive set of digital spatial data that encodes information about naturally occurring and constructed streamlines (<http://nhd.usgs.gov/>). NHD is a national map on surface water component used by geographic information systems (GIS). The water components contain lakes, streams, canals, and so on, which are combined together as the surface-water systems. Those features in the NHD are organized into polygons, lines and points. Perennial stream are abstracted from the NHD flowlines. NHD flowlines are lots of shorter segments of stream lines broken by stretching from confluence to confluence. Those segments are linked together to form the stream network.

The map scale of the high-resolution NHD is 1:24,000. All flow lines have been classified as perennial, intermittent, ephemeral streams, and others. The stream classification is based on digitizing the “blue line mapping” and stream symbolization on U.S. Geological Survey (USGS) 7.5 min quadrangle topographic maps where the perennial stream as blue lines while dashed blue lines are considered as intermittent stream, which is based on regional models and hydrologic systems.

The blue-line mapping and perennial and ephemeral or intermittent classifications on topographic maps used in the NHD are based on aerial photo interpretation and have been extensively verified by field reconnaissance by the USGS at the time the map was compiled or revised (*Simley, 2003*). Errors may occur in the process of digitally capturing the topographic map information and incorporating it into the NHD flow lines. Climate change, landscape change, human engineering and other variables present opportunities for improvement (*Simley, 2007*).

In the high-resolution NHD, each feature has its unit code, called Fcodes, which are five-digit integer value comprised of the feature type and the combinations of characteristics and values. In the dataset, streamlines are classified into perennial (46006), intermittent (46003), ephemeral streams (46007), and others. Some perennial streams with human interferences are classified as artificial path (55800), connector (33400), or others, as shown in Table 3.1. Therefore, these types of flow lines located in main channel should also be accounted into perennial streams when the total perennial stream length is computed. It should be noted that the value of total stream length, particularly for temporal (i.e., intermittent and ephemeral) streams, depends on the resolution of the map from which the streams were obtained (*Montgomery and*

*Dietrich, 1988*). The temporal streams in the NHD are usually underestimated since the small order headwater streams are usually not accounted due to the limited spatial resolution of the topographic map. However, this research is focused on perennial stream which is much more reliable than temporal streams in the NHD dataset.

Table 3.1. The types of flow lines (Fcodes) contained in perennial stream length calculation in NHD

Name	Fcodes
Connector	33400
Canal/Ditch	33600
Canal/Ditch: Canal/Ditch Type = Aqueduct	33601
Lake/Pond: Hydrographic Category = Perennial	39004
Lake/Pond: Hydrographic Category = Perennial; Stage = Average Water Elevation	39009
Lake/Pond: Hydrographic Category = Perennial; Stage = Normal Pool	39010
Lake/Pond: Hydrographic Category = Perennial; Stage = Date of Photography	39011
Lake/Pond: Hydrographic Category = Perennial; Stage = Spillway Elevation	39012
Pipeline: Pipeline Type = Aqueduct; Relationship to Surface = Elevated	42802
Pipeline: Pipeline Type = General Case; Relationship to Surface = Elevated	42806
Pipeline: Pipeline Type = Penstock; Relationship to Surface = Elevated	42810
Pipeline: Pipeline Type = Siphon	42813
Reservoir: Reservoir Type = Water Storage; Construction Material = Earthen; Hydrographic Category = Perennial	43615
Reservoir: Reservoir Type = Water Storage; Hydrographic Category = Perennial	43621
Stream/River	46000
Stream/River: Hydrographic Category = Perennial	46006
Swamp/Marsh: Hydrographic Category = Perennial	46602
Artificial Path	55800

All streams for each subwatershed are obtained by cut the NHD flowline data according each subwatershed's boundary in GIS. Then select those line segments with the perennial stream Fcodes (46006), as well as other line segments located in main channels with Fcodes shown in Table 3.1. The perennial stream length ( $L_p$ ) for 185 study watersheds range from 0 km to 6456

km. Figure 3.10 gives the spatial distribution of perennial stream length for the 185 study watersheds and Figure 3.11 shows the histogram of perennial stream length for study watersheds. It is obviously that the perennial streams in eastern U.S are shorter than that in High Plains. And from Figure 3.11 most of the perennial streams are less than 2000 km.

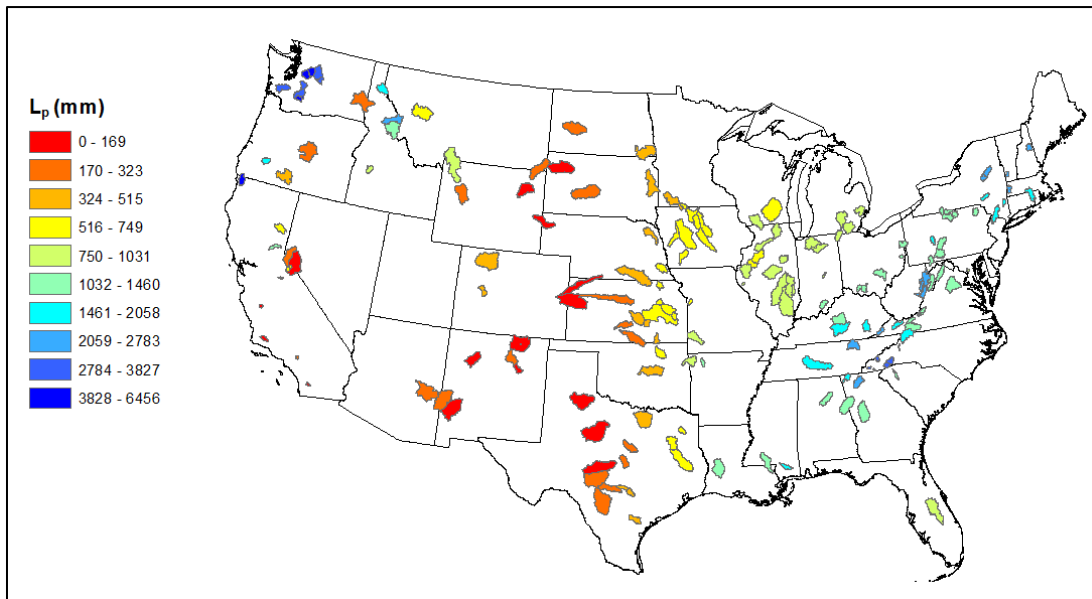


Figure 3.10. Spatial distribution of perennial stream length ( $L_p$ ) for the 185 study watersheds.

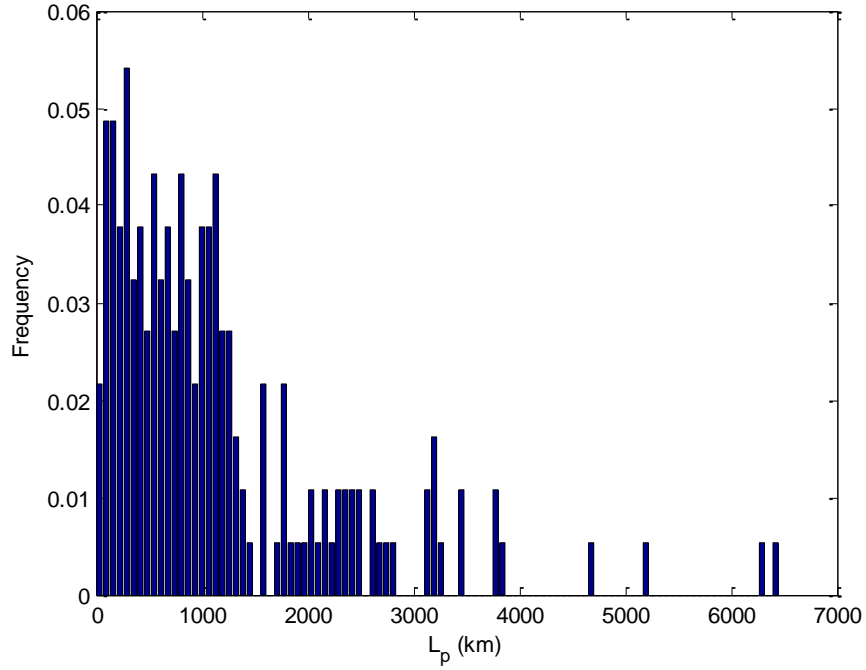


Figure 3.11. The histogram of perennial stream length ( $L_p$ ) for the 185 study watersheds.

### 3.1.3 Base Flow

Mean annual base flow is computed by conducting base flow separation using a one-parameter low-pass filter method (*Lyne and Hollick, 1979; Nathan and McMahon, 1990; Arnold and Allen, 1999; Lim et al., 2005*):

$$R_t = \alpha R_{t-1} + \frac{(1+\alpha)}{2} (Q_t - Q_{t-1}) \quad (1)$$

where  $R_t$  is the filtered direct runoff at time step  $t$ ;  $R_{t-1}$  is the filtered direct runoff at time step  $t-1$ ;  $\alpha$  is the filter parameter;  $Q_t$  is the total streamflow at time step  $t$ ;  $Q_{t-1}$  is the total streamflow at time step  $t-1$ .



The one-parameter low-pass filter method has no physical meaning. It comes from digital filter method which has been used to separate high frequency signal from low frequency signal in signal analysis and processing (Lyne and Hollick, 1979). Eckhardt (2005) suggested there is similar relationship between base flow separation and signal analysis and processing. The direct runoff can be associated with the high frequency signal, and the base flow can be associated with the low frequency signal. So, one-parameter low-pass filter method retains the low frequency part, which is the base flow, and filter out the high frequency part, the direct runoff. This method is fast, consistent and can avoid the subjective aspect of manual base flow separation. Figure 3.12 shows an example of the base flow separation for Snoqualmie River watershed in Washington with USGS gage 12149000 during two months period.

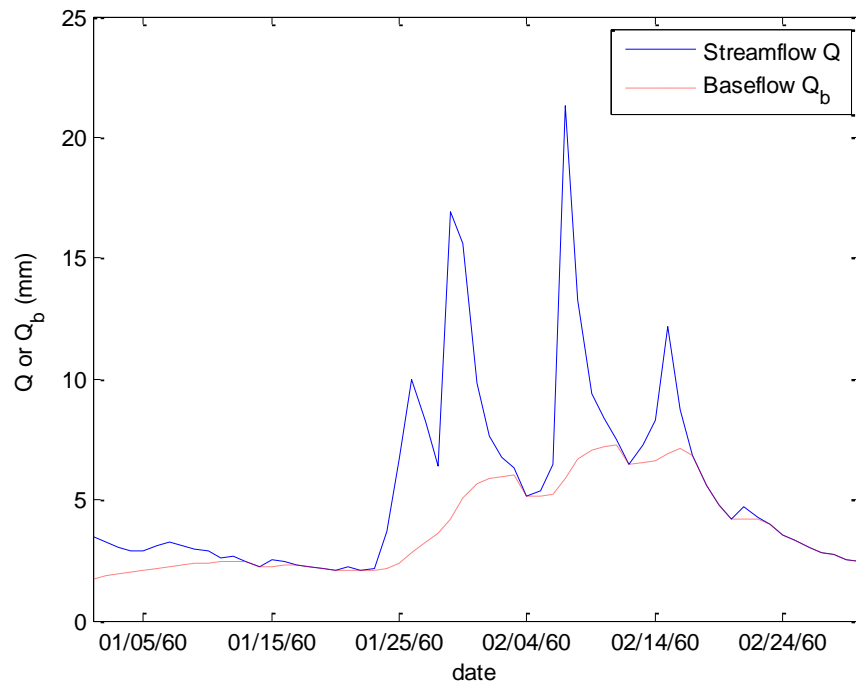


Figure 3.12. The base flow separation result for Snoqualmie River watershed, Washington with USGS gage 12149000 during January 1<sup>th</sup>, 1960 to March 1<sup>th</sup>, 1960.

The Web-based Hydrograph Analysis Tool (WHAT)

(<https://engineering.purdue.edu/~what/>) provides online tool for base flow separation by one-parameter low-pass filter method. This tool is used to obtain daily base flow for all the case study watersheds.

### 3.2 Budyko Framework

Based on datasets from a large number of watersheds, *Budyko* (1974) proposed a relationship between mean annual evaporation ratio ( $E/P$ ) and mean annual climate aridity index ( $E_p/P$ ):

$$\frac{E}{P} = \sqrt{\frac{E_p}{P} \left[ 1 - \exp\left(-\frac{E_p}{P}\right) \right] \tanh\left(\frac{1}{E_p/P}\right)} \quad (2)$$

where  $E$  is the mean annual evaporation.

As shown in Figure 3.13, evaporation ratio, which is captured by the Budyko curve, increases from humid to arid regions. The slope of the Budyko curve is steep in energy-limited regions (i.e.,  $E_p/P < 1$ ), and becomes flat in water-limited regions ( $E_p/P > 1$ ).

Other functional forms of Budyko-type curves have been developed for assessing long-term water balance (e.g., *Turc*, 1954; *Pike*, 1964; *Fu*, 1981; *Zhang et al.*, 2001; *Sankarasubramanian and Vogel*, 2002a; *Yang et al.*, 2008). One of the Budyko-type functions is the Turc-Pike equation:

$$\frac{E}{P} = \left[ 1 + \left(\frac{E_p}{P}\right)^{-v} \right]^{-1/v} \quad (3)$$

where  $v$  is the parameter that represents the effects of other factors such as vegetation, soil, and topography on the partitioning of precipitation.

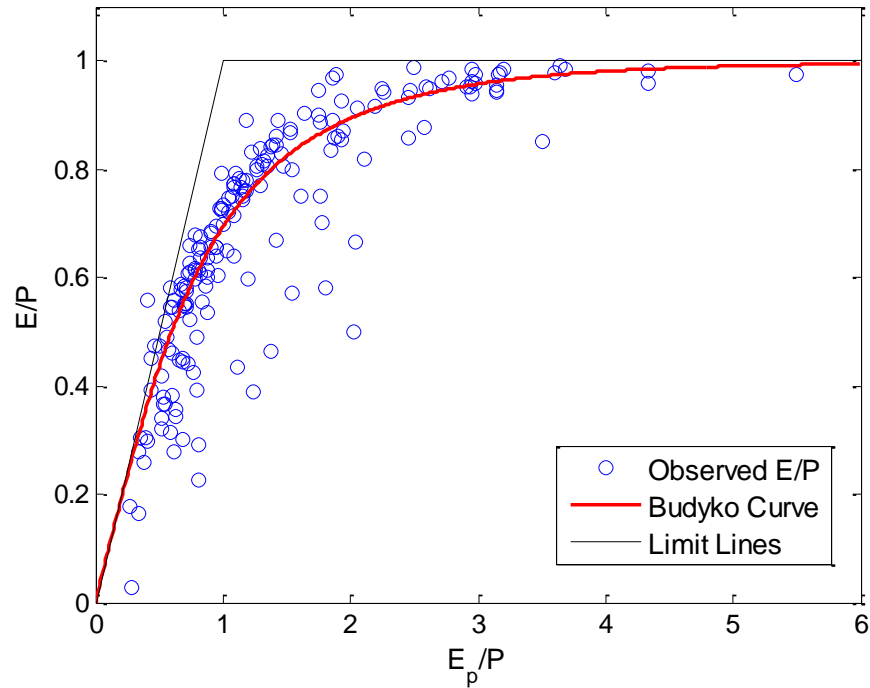


Figure 3.13. Comparison of observed evaporation ratio ( $E/P$ ) with estimates based on Budyko curve at the 185 study watersheds.

The mean annual precipitation, potential evaporation, and runoff ( $Q$ ) for the study watersheds are computed based on the available data of daily precipitation, runoff, and climatologic potential evaporation. Climate data is available during 1948-2003. Even though the general findings on climate control on perennial stream density is not affected by the selection of period for hydro-climatic data, the mean annual  $E/P$  and  $E_p/P$  during 1948-1970 are used considering the time period when the perennial stream data was constructed. As shown in Figure 3.13, the observed mean annual evaporation ratio for the study watersheds (i.e., blue circle) is along the Budyko curve (i.e., red line). The scatter of the data points in Figure 3.13 is caused by data uncertainty and other controlling factors such as climate seasonality, vegetation, soil, and topography (Milly, 1994; Zhang *et al.*, 2001; Donohue *et al.*, 2007; Yang *et al.*, 2007;

Yokoo *et al.*, 2008; Zhang *et al.*, 2008). At the mean annual scale, the steady-state condition can be assumed for water balance. Runoff coefficient ( $Q/P$ ) can be estimated by the complementary Budyko-type curve, i.e.,  $Q/P=1-E/P$ .

Similar to runoff coefficient, base flow coefficient, which is defined as the ratio of mean annual base flow ( $Q_b$ ) to precipitation, is also mainly controlled by climate aridity index. Base flow coefficients of the case study watersheds are plotted in Figure 3.14 as a function of climate aridity index. A complementary Turc-Pike curve is fitted to the observed data points:

$$\frac{Q_b}{P} = 1 - \left[ 1 + \left( \frac{E_p}{P} \right)^{-3.3} \right]^{-1/3.3} \quad (4)$$

The estimated value for the parameter  $\nu$  is 3.3 for the data points in Figure 3.14.

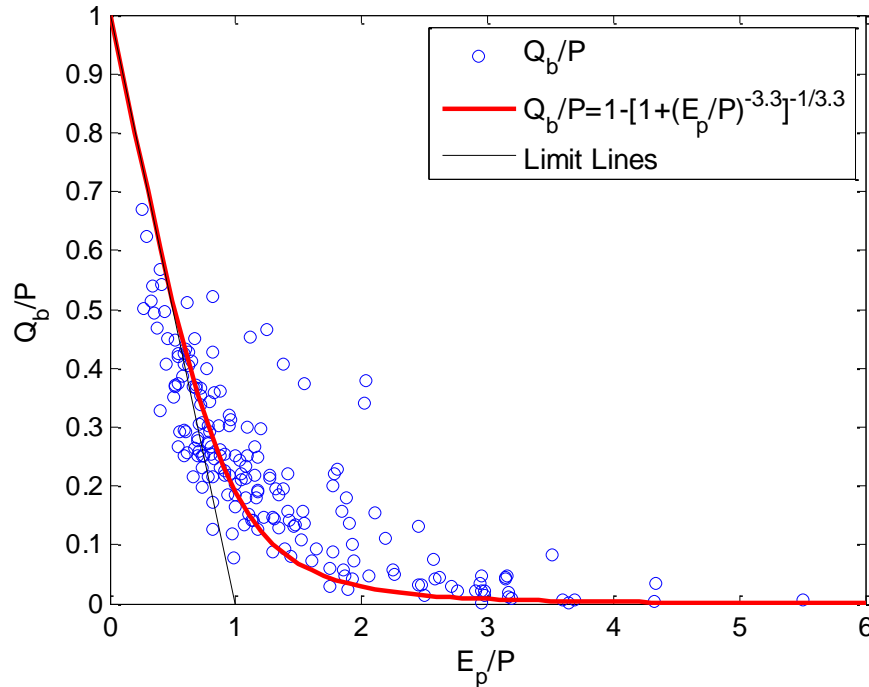


Figure 3.14.  $Q_b/P$  versus  $E_p/P$ , and the fitted complementary Turc-Pike curve.

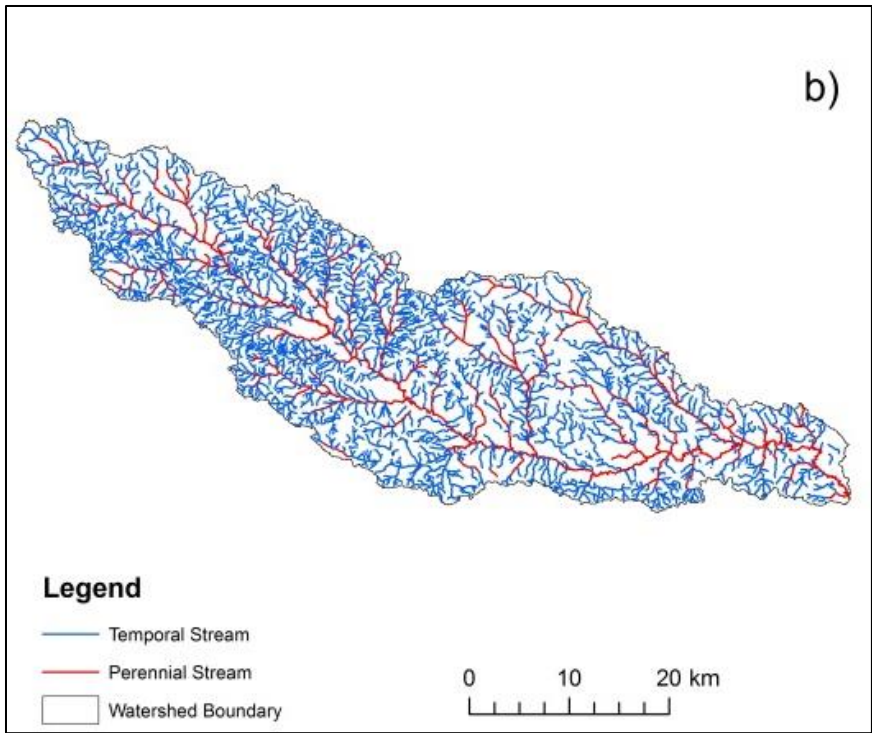
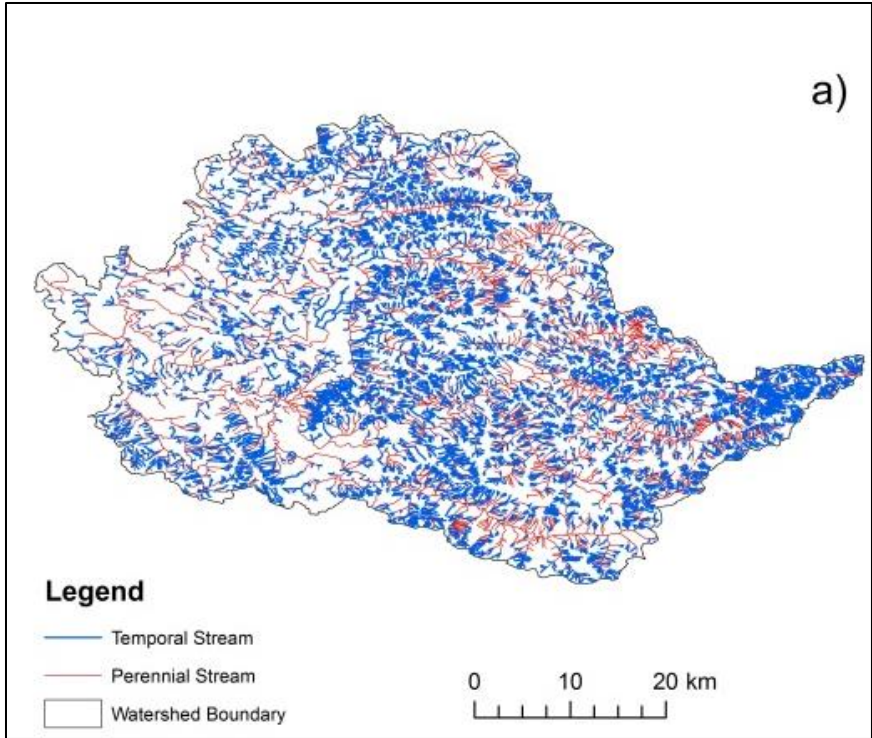
### 3.3 Perennial Stream Density as a Function of Climate Aridity Index

Generally, perennial stream density ( $D_p$ ) is higher in humid regions than that in arid regions. Perennial stream networks are mainly controlled by mean climate as well as other factors such as lithology and topography. The hydrologic function of perennial streams is to deliver runoff, particularly during low flow seasons when base flow is dominant. As discussed above, the pattern of  $Q_b/P$  can be captured by the complementary Budyko-type curve shown in equation (4). In this paper, perennial stream density as a function of climate aridity index and the correlation between  $D_p$  and  $Q_b/P$  are evaluated.

## CHAPTER 4: RESULTS AND DISCUSSIONS

### 4.1 Results

Perennial stream length and density are computed for each study watershed based on the NHD dataset. Figure 4.1 shows the perennial and temporal streams for four selected watersheds with different climate aridity index. The climate aridity index and perennial stream density for the Snoqualmie River watershed located in the State of Washington is 0.29 and 1.60 km/km<sup>2</sup>, respectively (Figure 4.1a). However, in the arid region of New Mexico ( $E_p/P=5.50$ ), the perennial stream density for the Arroyo Chico watershed is only 0.067 km/km<sup>2</sup> (Figure 4.1d). Figures 4.1b and 4.1c show the perennial stream network at the other two watersheds with climate aridity index of 0.70 and 1.77, respectively. Perennial stream densities decrease from energy-limited to water-limited regions.



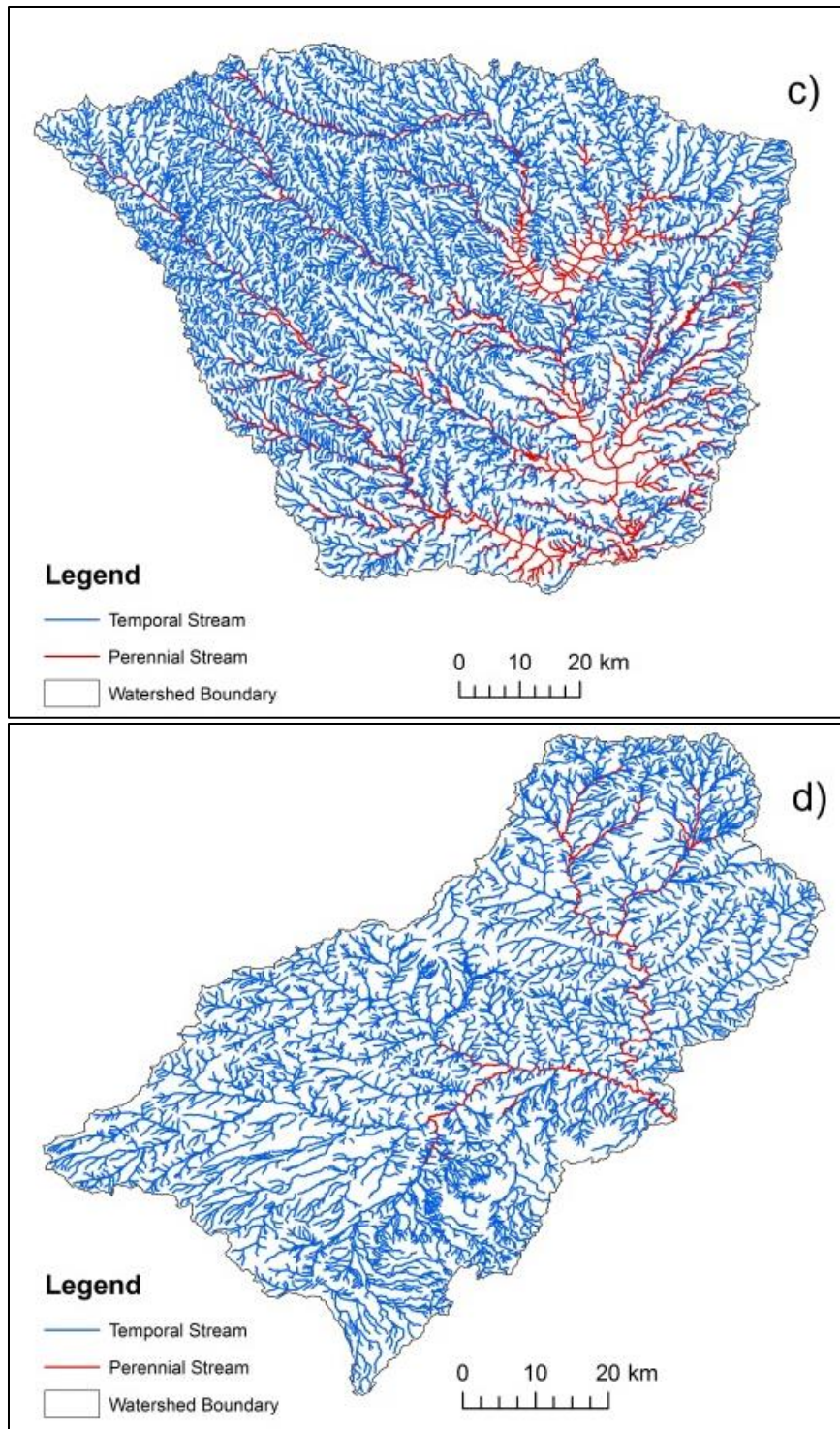


Figure 4.1. Temporal stream and perennial stream: a) Snoqualmie River watershed, Washington with USGS gage 12149000,  $E_p/P=0.29$ ,  $D_p=1.60 \text{ km}^{-1}$ ; b) Red Creek watershed, Mississippi with



USGS gage 02479300,  $E_p/P=0.70$ ,  $D_p=0.48 \text{ km}^{-1}$ ; c) Elm Fork Trinity River watershed, Texas with USGS gage 08055500,  $E_p/P=1.77$ ,  $D_p=0.27 \text{ km}^{-1}$ ; d) Arroyo Chico watershed, New Mexico with USGS gage 08340500,  $E_p/P=5.50$ ,  $D_p=0.067 \text{ km}^{-1}$ .

The spatial distribution and histogram of perennial stream densities for all the case study watersheds are shown in Figure 4.2 and Figure 4.3 respectively. As we can see, perennial stream densities are higher in the eastern U.S. and relatively lower in the High Plains. The minimum perennial stream density is  $0 \text{ km/km}^2$  and the maximum perennial stream density is  $1.59 \text{ km/km}^2$  over the 185 study watersheds. Most of the perennial stream densities are less than  $1 \text{ km/km}^2$ .

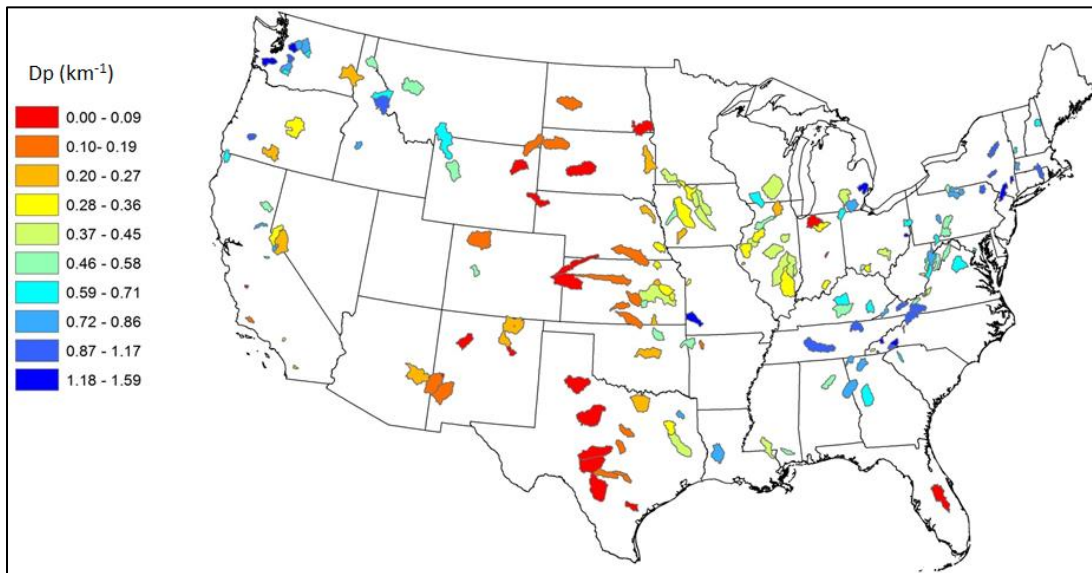


Figure 4.2. Spatial distribution of perennial stream densities ( $D_p$ ) for the 185 study watersheds.

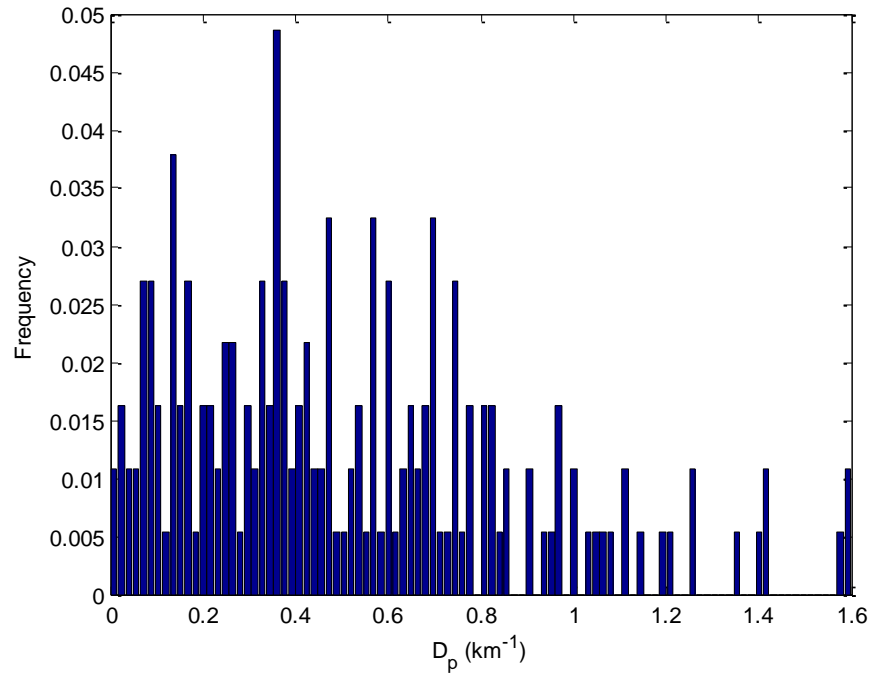


Figure 4.3. The histogram of perennial stream densities ( $D_p$ ) for the 185 study watersheds.

The perennial stream densities obtained from the NHD dataset are compared with the reported ones in the literature. *De Wit and Stankiewicz (2006)* reported the perennial stream densities in Africa and the values vary from 0 to 0.14  $\text{km}/\text{km}^2$ . In a small peatland headwater catchment in United Kingdom, the perennial stream density is 1.41  $\text{km}/\text{km}^2$  when water tables fall below 180 mm; but the total drainage density is 29.98  $\text{km}/\text{km}^2$  when the stream network is fully expanded (*Goulsbra et al., 2012*). The perennial stream density in the Turnhole Bend Groundwater Basin in Kentucky is reported in values ranging from 0.24  $\text{km}/\text{km}^2$  to 1.13  $\text{km}/\text{km}^2$ . *Johnston and Shmagin (2008)* reported that the average perennial stream density of several watersheds located in the Great Lakes is 0.42  $\text{km}/\text{km}^2$ . Perennial stream density in the Northern Rockies Eco-region is relatively high and the values reported range from 0.9  $\text{km}/\text{km}^2$  to 1.2  $\text{km}/\text{km}^2$  (*McIntosh et al., 1995*). *Wigington et al. (2005)* reported that perennial stream density

of agricultural watersheds in western Oregon varies from 0.24 km/km<sup>2</sup> to 0.66 km/km<sup>2</sup> even though the total stream density varies from 2.90 km/km<sup>2</sup> to 8.00 km/km<sup>2</sup>. The perennial stream density for the four case study watersheds located in western Oregon are 0.1 km/km<sup>2</sup> (USGS gage 14308000), 0.26 km/km<sup>2</sup> (USGS gage 11497500), 0.29 km/km<sup>2</sup> (USGS gage 14080500), and 0.67 km/km<sup>2</sup> (USGS gage 11532500) as shown in Figure 4.2. The magnitude of perennial stream density computed based on the NHD dataset is consistent to these reported values in the literature.

To explore the climate control on perennial streams, perennial stream densities of all the study watersheds are plotted as a function of climate aridity index (Figure 4.4). The blue circles represent the NHD-based perennial stream density which monotonically decreases with climate aridity index. The narrow-banded data cloud shows the strong dependence of perennial stream density on  $E_p/P$ . *De Wit and Stankiewicz* (2006) studied the mean annual precipitation control on perennial stream density in Africa, and proposed a non-monotonic relationship. Annual precipitation has usually been the main focus in studies of climate control on drainage density (e.g., *Abrahams and Ponczynski*, 1984). To include the effect of energy, *PE* index proposed by *Thornthwaite* (1931) contains both precipitation and actual evaporation which is implicitly related to temperature (*Moglen et al.*, 1998). However, from the perspective of water balance, the hydrologic basis of the *PE* index is not as strong as that of the climate aridity index proposed by *Budyko* (1958). *Gregory* (1976) compared the pattern of total drainage density as a function of climate aridity index, but no explicit pattern was discovered. The reason is that the dependence of temporal streams on mean climate is not strong as perennial streams. As we expect, a monotonic trend is identified for perennial stream density as a function of climate

aridity index in this study. An inversely proportional function is proposed to fit the data points in Figure 4.4

$$D_p = \frac{k}{E_p/P} \quad (5)$$

where the coefficient  $k$  represents the perennial stream density for watersheds with balanced water and energy supply ( $E_p/P=1$ ), and the value of  $k$  is  $0.44 \text{ km}^{-1}$  based on the fitted curve.

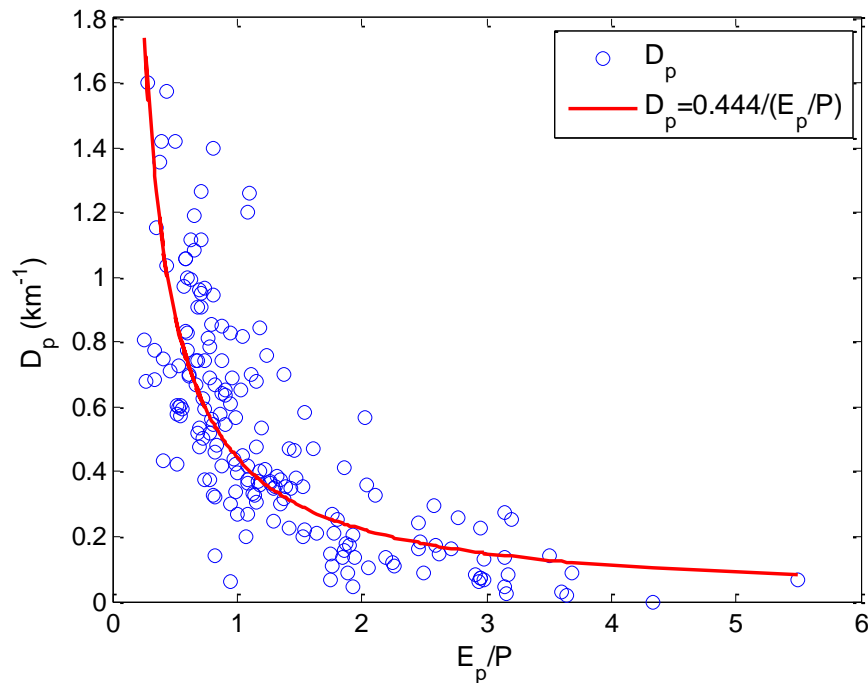


Figure 4.4. NHD-based perennial stream density,  $D_p$  ( $\text{km}^{-1}$ ), and the fitted line are plotted as a function of climate aridity index ( $E_p/P$ ).

Since perennial stream is defined as the active stream during drought periods when base flow dominates the streamflow, perennial stream density may be correlated with base flow coefficient. As shown in Figure 4.5, the correlation between perennial stream density and base flow coefficient is indeed strong, and the correlation coefficient between them is 0.74. Furthermore, since climate aridity index is the first order control on both  $Q_b/P$  (Figure 3.14) and

$D_p$  (Figure 4.4), similarity exists between base flow coefficient and perennial stream density in the dependence on mean annual climate aridity index.

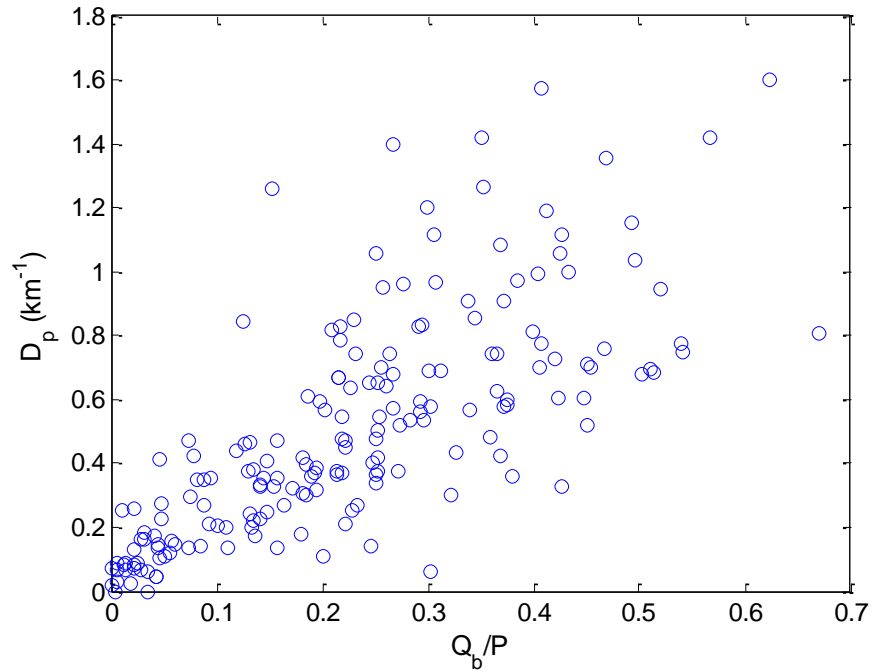


Figure 4.5. The correlation coefficient between perennial stream density ( $D_p$ ) and base flow coefficient ( $Q_b/P$ ) is 0.74.

## 4.2 Discussions

### 4.2.1 Perennial, Intermittent, Ephemeral, and Total Stream Densities

The Abrahams curve (Figure 4.6) represents the dependence of total drainage density ( $D_d$ ) on  $PE$  index which is computed by:

$$PE = 10 \sum_{m=1}^{12} \frac{P_m}{E_{p_m}} \quad (6)$$

where  $P_m$  and  $E_{p_m}$  are mean monthly precipitation and potential evaporation, respectively (Thornthwaite, 1931). As shown in Figure 4.6,  $D_d$  decreases and then increases with  $PE$  index (Abrahams, 1984). The relationship between  $PE$  index and  $E_p/P$  for the case study watersheds is

shown in Figure 4.7. Higher  $PE$  index is corresponding to lower  $E_p/P$ , and the correlation coefficient between  $PE$  and  $E_p/P$  is  $-0.73$ .

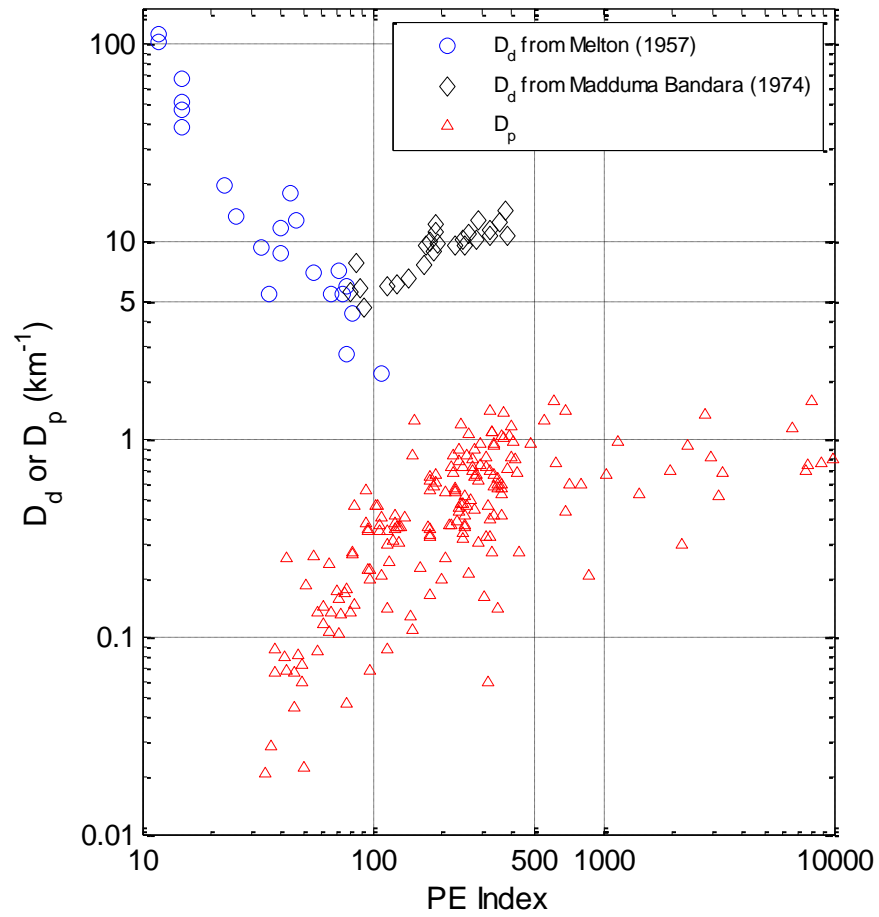


Figure 4.6. Total drainage density (Abraham, 1984) and perennial stream density as a function of  $PE$  index.

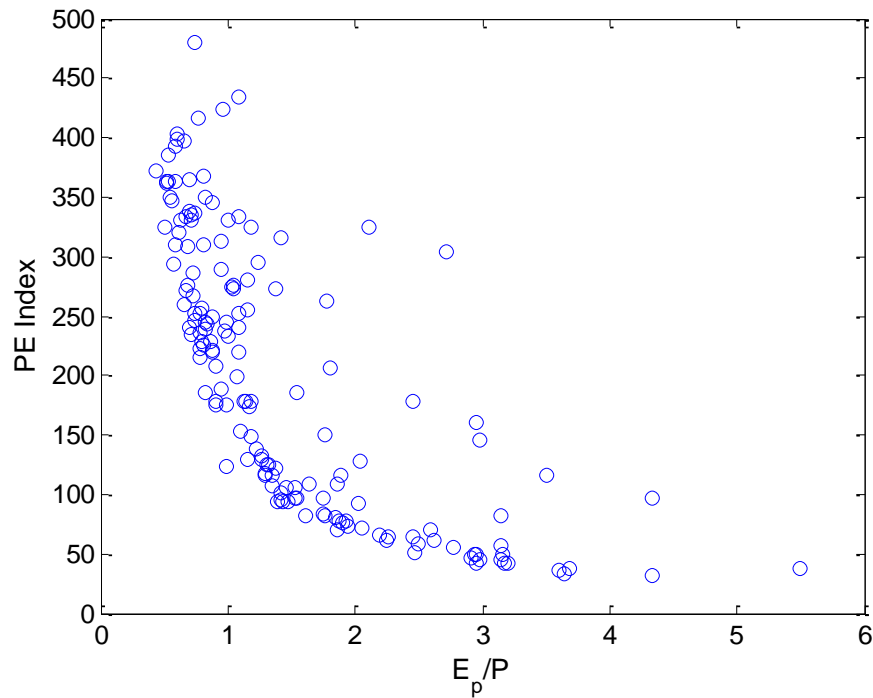


Figure 4.7. The correlation between  $PE$  index and climate aridity index ( $E_p/P$ ) for the 160 study watersheds with  $PE$  index less than 500.

To explore the contribution of perennial stream density to total drainage density reported by *Abrahams* (1984), perennial stream densities for the case study watersheds are added to the *Abrahams* curve in Figure 4.6. As we can see, perennial stream density increases with  $PE$  index. Perennial stream density is only a small portion of the total drainage density, and the trend of intermittent and ephemeral streams dominates that of total drainage density. However, perennial stream density contributes the increasing trend of total drainage density when  $PE$  index is higher than 100. Therefore, the findings on perennial stream density in this study do not contradict with the *Abrahams* curve.

As an alternative to the tradeoff between runoff erosion and resistance by vegetation, the observed non-monotonic trend of total drainage density as a function of  $PE$  index may be

explained by the runoff generation at different temporal scales (Figure 4.8). Definitions of perennial, intermittent and ephemeral streams are based on the streamflow duration in each river segment. Perennial stream is defined as the active stream even in drought periods. Therefore, mean climate control on perennial stream density and base flow coefficient is similar as discussed earlier. Intermittent stream is defined as seasonally active ones, and intermittent stream density ( $D_i$ ) may be related to the seasonal water balance. Ephemeral stream density ( $D_e$ ) is corresponding to high flows corresponding to extreme rainfall events. To fully reveal the co-evolution of total stream density and water balance at various temporal scales, the patterns of  $D_i$  and  $D_e$  as a function of  $E_p/P$  need to be further quantified in the future when accurate data is available.



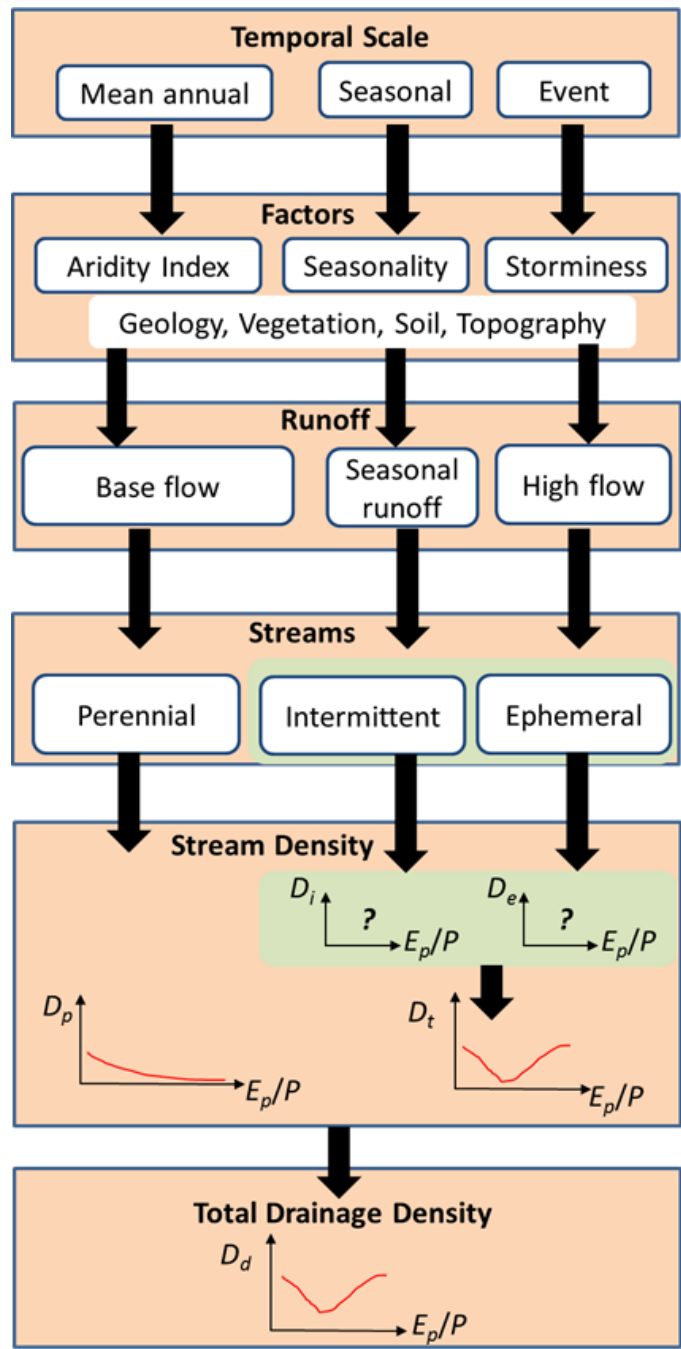


Figure 4.8. Perennial, intermittent and ephemeral streams and runoff generation from mean annual to seasonal and to event scales.

#### 4.2.2 Normalized Perennial Stream Density

In order to compare the similarity of climate control on base flow and perennial stream in the Budyko framework, perennial stream density needs to be converted into a dimensionless number like the base flow coefficient. The perennial stream density in each watershed is then normalized by the maximum potential perennial stream density denoted as  $D_p^*$ . The normalized perennial stream density,  $D_p/D_p^*$ , can be plotted in the Budyko framework and compared with the complementary Budyko-type curve. However, it is a challenge to identify the maximum potential perennial stream density in each watershed. In this study, the total temporal and perennial stream density obtained from the NHD dataset is used for  $D_p^*$ . It should be noted that the NHD dataset is based on topographic maps equivalent to 30 m DEM. Total drainage densities are smaller than the values in Figure 4.6, and there is no obvious pattern in the relationship between the total density of perennial and temporal streams from the NHD and  $PE$  index or  $E_p/P$ .

The normalized perennial stream density is plotted in Figure 4.9 as a function of  $E_p/P$ . The red line in Figure 4.9 is the fitted Turc-Pike equation for base flow coefficient shown in Figure 3.14. Data points for  $D_p/D_p^*$  is a little bit above the red line. Considering the uncertainty of datasets and potential underestimation of  $D_p^*$ , the similarity between  $D_p/D_p^*$  and  $Q_b/P$  as a function of  $E_p/P$  is promising based on the case study watersheds. The limit lines for base flow coefficient are represented by black lines in Figure 4.9. Due to the uncertainty in the hydro-climatic data, several data points ( $E/P$ ) are located above the limit line, i.e., the 1:1 line shown in Figure 3.13. However, more data points for  $D_p/D_p^*$  are located below the limit line in Figure 4.9. Besides uncertainty of perennial stream data in the NHD dataset, the value of  $D_p^*$  can also affect

the position of these points. Long-term climate may not be the main controls in some special watersheds and perennial stream density is high due to geology and lithology. The data points in Figure 4.9 may be not necessarily above the limit line, i.e.,  $D_p/D_p^* > 1 - E_p/P$ . Even though the similarity exists in the base flow coefficient and perennial stream density dependence on long-term mean climate, the controls of other factors on water balance and perennial stream may be different.

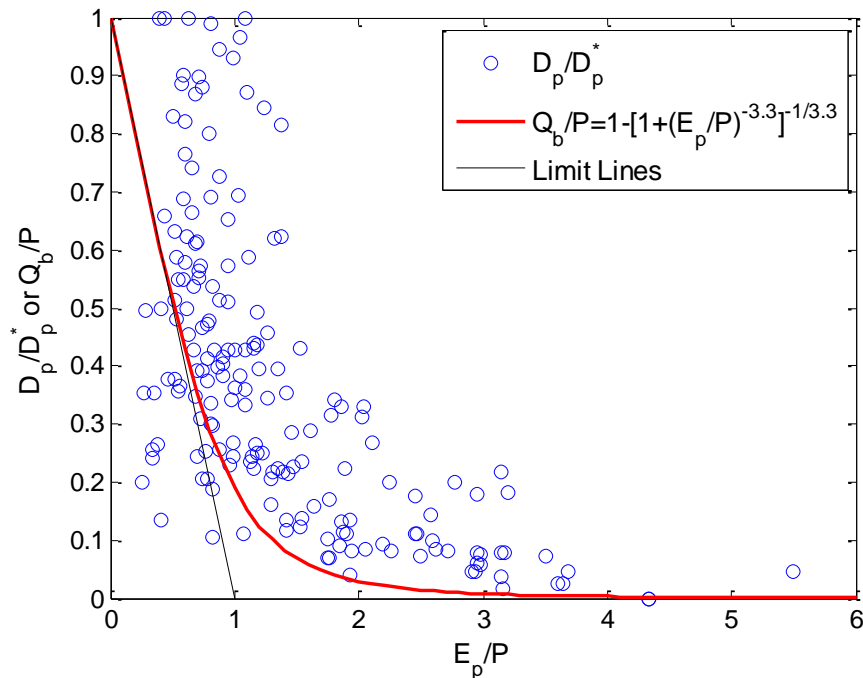


Figure 4.9.  $D_p/D_p^*$  versus  $E_p/P$  and the fitted complementary Turc-Pike curve for  $Q_b/P$  versus  $E_p/P$ .

### 4.2.3 Impact of Slope on Perennial Stream Density

Besides mean climate, the topographic control on perennial stream density is investigated here. The average slope for each watershed is computed by using the 90-m DEM SRTM data for North America downloaded from [http://dds.cr.usgs.gov/srtm/version2\\_1/SRTM3/](http://dds.cr.usgs.gov/srtm/version2_1/SRTM3/). Figure 4.10

shows the relationship between perennial stream density and slope by percentage. Generally, high perennial stream density is associated with higher slope, but the dependence is not strong as climate aridity index shown in Figure 4.4. It should be noted that slope is also related to climate aridity index in certain levels. Therefore, mean annual climate is the first order control on perennial stream density like rainfall partitioning, but other factors such as slope may be the second order control.

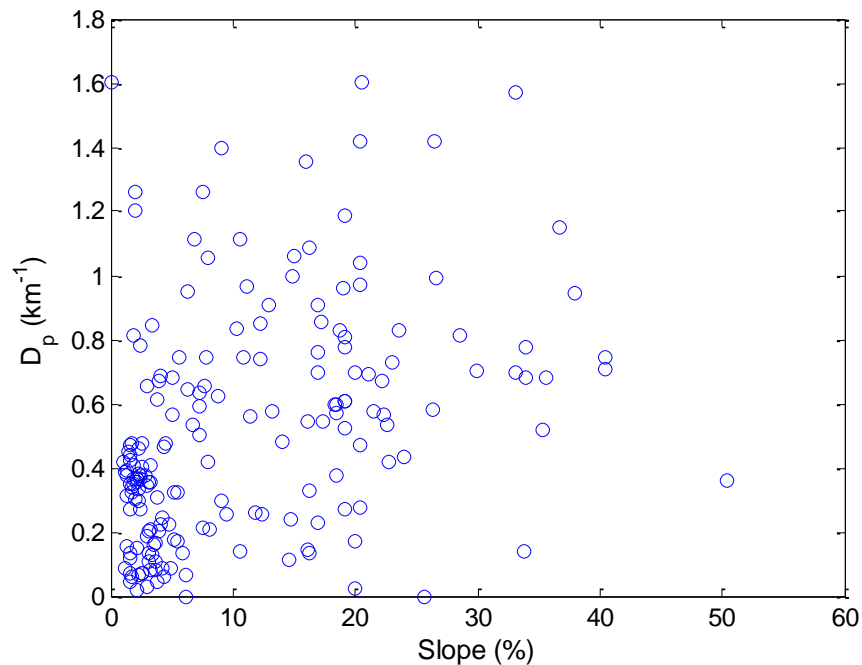


Figure 4.10. Perennial stream density versus slope (%) for the 185 study watersheds.

#### **4.2.4 Application of the Relationship between Perennial Stream Density and Climate Aridity Index**

One of the purposes for this research is to develop a simple model to predict perennial stream density. For example, *De Wit and Stankiewicz* (2006) applied the step-wise linear relationship between mean annual precipitation and perennial stream density to assess the

climate change impact on perennial stream density in Africa. In this paper, an inversely proportional function is developed to predict perennial stream densities based on climate aridity index. The scatters in Figure 4.4 reflect the impact of other factors on perennial stream density. Empirical relationships between the values of parameter  $k$  and the other factors can be constructed so that perennial stream density can be predicted more accurately. In global hydrological models, an estimate of the perennial stream density for each grid cell (e.g.,  $0.5^\circ \times 0.5^\circ$ ) is needed in order to model the local groundwater level and the groundwater discharge (*Van Beek and Bierkens, 2008; Wu et al., 2011*). The findings from this research will provide a framework to modeling perennial stream density for macroscale hydrological model development.

## CHAPTER 5: CONCLUSIONS AND RECOMMENDATIONS

The observed pattern of perennial stream density can be explained by the hydrologic functions of perennial streams. Climate aridity index is the first order control on perennial stream density, and an inversely proportional function is used to model the dependence of perennial stream density on climate aridity index. Therefore, the perennial stream density is one component of co-evolution of climate, vegetation, soil, and landscape at the mean annual scale. Furthermore, perennial stream density is strongly correlated with base flow coefficient which is the ratio of mean annual base flow to precipitation. Similarity may exist between the dependences of normalized perennial stream density and base flow coefficient on climate aridity index and the climate control is quantified by complementary Budyko-type curves.

In this thesis, the first order control (i.e., mean climate) on perennial stream density is the focus. The scatters of the normalized perennial stream density in the Budyko framework are due to other factors such as vegetation type and coverage, soil, topography, and geology. Future efforts can investigate the impact of these factors on the perennial stream density from the perspective of hydrologic functions in the Budyko framework. The maximum perennial stream density, which is the normalization factor, is estimated based on the NHD dataset. The maximum perennial stream density for individual watershed is open for further investigation. To fully reveal the co-evolution between water balance and total drainage density, intermittent and ephemeral stream densities need to be quantified, respectively.

## REFERENCES

- Abrahams, A. D. (1984), Channel Networks: A Geomorphological Perspective, *Water Resour. Res.*, 20(2), 161–188, doi:10.1029/WR020i002p00161.
- Abrahams, A. D., and J. J. Ponczynski (1984), Drainage density in relation to precipitation intensity in the USA, *J. Hydrol.*, 75(1–4), 383–388.
- Arnold, J. G., and P. M. Allen (1999), Validation of automated methods for estimating baseflow and groundwater recharge from stream flow records. *Journal of American Water Resources Association*, 35:411-424.
- Berger, K. P., and D. Entekhabi (2001), Basin hydrologic response relations to distributed physiographic descriptors and climate, *J. Hydrol.*, 47 (3–4), 169–182.
- Bhagwat, S. B. (2009), *Foundation of Geology*, 322, Global Vision Publishing House, India.
- Budyko, M. I. (1958), *The Heat Balance of the Earth's Surface*, translated from Russian by N. A. Stepanova, 259 pp., U.S. Dep. of Commer., Washington, D.C..
- Budyko, M. I. (1974), *Climate and Life*, 508 pp., Academic Press, New York.
- Carlston, C. W. (1963), *Drainage Density and Stream Flow*: U.S. Geological Survey Professional Paper No. 422-C, pp. 1–8.
- Collins, D. B. G., and R. L. Bras (2010), Climatic and ecological controls of equilibrium drainage density, relief, and channel concavity in dry lands, *Water Resour. Res.*, 46, W04508, doi:10.1029/2009WR008615.

- Day, D. G. (1978), Drainage density changes during rainfall, *Earth Surfaces and Processes*, 3(3), 319-326.
- De Wit, M., and J. Stankiewicz (2006), Changes in surface water supply across Africa with predicted climate change, *Science*, 311(5769), 1917–21.
- Donohue, R. J., M. L. Roderick, and T. R. McVicar (2007), On the importance of including vegetation dynamics in Budyko's hydrological model, *Hydrol. Earth Syst. Sci.*, 11, 983-995.
- Duan, Q., et al. (2006), The Model Parameter Estimation Experiment (MOPEX): An overview of science strategy and major results from the second and third workshops, *J. Hydrol.*, 320, 3–17.
- Fu, B. P. (1981), On the calculation of the evaporation from land surface, *Scientia Atmospherica Sinica*, 5(1), 23–31 (in Chinese).
- Gerrits, A. M. J., H. H. G. Savenije, E. J. M. Veling, and L. Pfister (2009), Analytical derivation of the Budyko curve based on rainfall characteristics and a simple evaporation model, *Water Resour. Res.*, 45, W04403, doi:10.1029/2008WR007308.
- Gregory, K. J. (1976), Drainage networks and climate, in *Geomorphology and Climate*, edited by E. Derbyshire, pp. 289-315, John Wiley, New York.
- Harman, C. J., P. A. Troch, and M. Sivapalan (2011), Functional model of water balance variability at the catchment scale: 2. Elasticity of fast and slow runoff components to precipitation change in the continental United States, *Water Resour. Res.*, 47, W02523, doi:10.1029/2010WR009656.



- Hedman, E. R., and W. R. Osterkamp (1982), Stream flow characteristics related to channel geometry of streams in western United States. USGS Water-Supply paper 2193, 17.
- Hewlett, J.D. (1982), Principles of Forest Hydrology, *University of Georgia Press*, Athens, Ga, 183.
- Horton, R. E. (1932), Drainage basin characteristics, *Eos Trans.*, 13, 350-361.
- Horton, R. E. (1945), Erosional development of streams and their drainage basins: hydro-physical approach to quantitative morphology, *Geological Society of America Bulletin*, 56(3), 275–370.
- Hunrichs, R. A. (1983), Identification and classification of perennial streams of Arkansas, U.S. Geological Survey, *Water Resources Investigations Report 83-4063*.
- Ivkovic, K. M. (2009), A top-down approach to characterise aquifer-river interaction processes, *J. Hydrol.*, 365, 145-155.
- Kelson, K. I., and S. G. Wells (1989), Geologic influences on fluvial hydrology and bedload transport in small mountainous watersheds, northern New Mexico, USA, *Earth Surf. Processes Landforms*, 14, 671–690.
- Lim, K. J., B. A. Engel, Z. Tang, and J. Choi (2006), AUTOMATED WEB GIS BASED HYDROGRAPH ANALYSIS TOOL, *WHAT 1*, 1397, 1407–1416.
- Lyne, V., and M. Hollick (1979), Stochastic time-variable rainfall-runoff modeling, In: Proc. Hydrology and Water Resources Symposium, Perth, 89-92, Inst. Of Engrs. Australia.

- Madduma Bandara, C. M. (1974), Drainage density and effective precipitation, *J. Hydrol.*, 21, 187-190.
- McIntosh B. A., J. R. Sedell, R. F. Thurow, S. E. Clarke, and G. L. Chandler (1995), Historical changes in pool habitats in the Columbia River Basin, *Report to the Eastside Ecosystem Management Project*, Walla Walla, WA.
- Meinzer, O. E. (1923), Outline of ground-water hydrology, with definitions. Washington, DC: US Geological Survey, *Water Supply Paper 494*.
- Melton, M. A. (1957), An analysis of the relations among elements of climate, surface properties, and geomorphology, Tech. Rep. 11, Off. Nav. Res. Proj. 389-042, Dep. of Geol., Columbia Univ., New York.
- Merz, R. and G. Blöschl (2008), Flood frequency hydrology: 1. Temporal, spatial, and causal expansion of information, *Water Resour. Res.*, 44, W08432, doi:10.1029/2007WR006744.
- Milly, P. C. D. (1994), Climate, soil water storage, and the average annual water balance, *Water Resour. Res.*, 30, 2143-2156.
- Moglen, G. E., E. A. B. Eltahir, and R. L. Bras (1998), On the sensitivity of drainage density to climate change, *Water Resour. Res.*, 34(4), 855–862.
- Montgomery, D. R., and W. E. Dietrich (1988), Where do channels begin? *Nature*, 336, 232–234.
- Nahatan, R. J., and T. A., McMahon (1990), Evaluation of automated techniques for baseflow and recession analysis, *Wat. Resour. Res.*, 26, 1465-1473.

- Pallard, B., A. Castellarin, and A. Montanari (2009), A look at the links between drainage density and flood statistics, *Hydrol. Earth Syst. Sci.*, 13, 1019-1029.
- Paybins, K.S. (2003), Flow origin, drainage area, and hydrologic characteristics for headwater streams in the mountaintop coalmining region of southern West Virginia, 2000-01, USGS Water Resources Investigations Report, 02-4300. 20.
- Perron J. T., J. X. Mitrovica, M. Manga, I. Matsuyama, and M. A. Richards (2007), Evidence of an ancient martian ocean in the topography of deformed shorelines, *Nature*, 447, 840-843.
- Pike, J. G. (1964), The estimation of annual runoff from meteorological data in a tropical climate, *J. Hydrol.*, 2, 116– 123.
- Ritter, M. E. (2006), *The Physical Environment: an Introduction to Physical Geography*, data visited: [http://www4.uwsp.edu/geo/faculty/ritter/geog101/textbook/title\\_page.html](http://www4.uwsp.edu/geo/faculty/ritter/geog101/textbook/title_page.html)
- Sankarasubramanian, A. and R. M. Vogel (2002a), Annual hydroclimatology of the United States, *Water Resour. Res.*, 38, 1083, doi:10.1029/2001WR000619.
- Sankarasubramanian, A., and R. M. Vogel (2002b), Comment on Paper “Basin hydrologic response relations to distributed physiographic descriptors and climate”, *J. Hydrol.*, 263, 257–261.
- Simley, J. (2003), National Hydrography Dataset Newsletter, U.S. Geological Survey Report, 2(7).
- Simley, J. (2006), National Hydrography Dataset Newsletter, U.S. Geological Survey Report, 5(6).

- Simley, J. (2007), National Hydrography Dataset Newsletter, U.S. Geological Survey Report, 6(11).
- Sivapalan, M. (2005), Pattern, processes and function: elements of a unified theory of hydrology at the watershed scale. In: Anderson, M. (ed.) Encyclopedia of hydrological sciences. London: John Wiley, pp. 193–219.
- Sivapalan, M., M. A. Yaeger, C. J. Harman, X. Xu, and P. A. Troch (2011), Functional model of water balance variability at the catchment scale: 1. Evidence of hydrologic similarity and space-time symmetry, *Water Resour. Res.*, 47, W02522, doi:10.1029/2010WR009568.
- Stringer, J. C. Perkins, (2001), Kentucky Forest Practice Guidelines for Water Quality Management, University of Kentucky., Coop. Ext. Serv., Dept. of For. FOR-67, 111.
- Svec, J. R., R. K. Kolka, and J. W. Stringer (2005). Defining perennial, intermittent, and ephemeral channels in Eastern Kentucky: Application to forestry best management practices. *Forest Ecology and Management*, 214(1-3), 170–182. doi:10.1016/j.foreco.2005.04.008
- Texas Forest Service. (2000), Texas Forestry Best Management Practices, available from: <http://txforestservicetamu.edu/uploadedfiles/sustainable/bmp/bmpbookindd.pdf>.
- Thornthwaite, C. (1931), The climates of North America according to a new classification, *Geogr. Rev.*, 21, 633–655.
- Turc, L. (1954), Le bilan d'eau des sols: Relation entre les precipitations, l'évaporation et l'écoulement, *Ann. Agron.*, 5, 491-569.
- Van Beek, L. P. H., and M. F. P. Bierkens (2008), The global hydrological model PCR-Globwb: conceptualization, parameterization and verification, Report Department of Physical

Geography, Utrecht University, Utrecht, The Netherlands,  
<http://vanbeek.geo.uu.nl/supinfo/vanbeekbierkens2009.pdf>.

- Wagener, T., M. Sivapalan, P. Troch, and R. Woods (2007), Watershed classification and hydrologic similarity, *Geography Compass*, 1(4), 901.
- Wang D. and M. Hejazi (2011), Quantifying the relative contribution of the climate and direct human impacts on mean annual streamflow in the contiguous United States, *Water Resour. Res.*, 47, W00J12, doi:10.1029/2010WR010283.
- Wang, D. and L. Wu (2013), Similarity of climate control on base flow and perennial stream density in the Budyko framework, *Hydrol. Earth Syst. Sci.*, 17(1), 315-324, doi:10.5194/hess-17-315-2013.
- Wang, D. and N. Alimohammadi (2012), Responses of annual runoff, evaporation and storage change to climate variability at the watershed scale, *Water Resour. Res.*, 48, W05546, doi:10.1029/2011WR011444.
- Washburn. E, C. Carr, and S. Diveley (2007), New Guidance Narrows Federal Regulation of Some Wetlands, Streams and Ditches, Client Alert, Morrison Foerster.
- Wigington, P. J. , T. J. Moser, and D. R. Lindeman (2005), Stream network expansion: a riparian water quality factor, *Hydrol. Process.*, 19, 1715-1721.
- Wu, H., J. S. Kimball, N. Mantua, and J. Stanford (2011), Automated upscaling of river networks for macroscale hydrological modeling, *Water Resour. Res.*, 47, W03517, doi:10.1029/2009WR008871.

- Yang, D., F. Sun, Z. Liu, Z. Cong, G. Ni, and Z. Lei (2007), Analyzing spatial and temporal variability of annual water-energy balance in nonhumid regions of China using the Budyko hypothesis, *Water Resour. Res.*, 43, W04426, doi:10.1029/2006WR005224.
- Yang, H., D. Yang, Z. Lei, and F. Sun (2008), New analytical derivation of the mean annual water-energy balance equation, *Water Resour. Res.*, 44, W03410, doi:10.1029/2007WR006135.
- Yokoo, Y., M. Sivapalan, and T. Oki (2008), Investigating the roles of climate seasonality and landscape characteristics on mean annual and monthly water balances, *J. Hydrol.*, 357, 255-269.
- Zhang, L., N. Potter, K. Hickel, Y. Zhang, and Q. Shao (2008), Water balance modeling over variable time scales based on the Budyko framework – Model development and testing, *J. Hydrol.*, 360, 117-131.
- Zhang, L., W. R. Dawes, and G. R. Walker (2001), Response of mean annual evapotranspiration to vegetation changes at watershed scale, *Water Resour. Res.*, 37(3), 701–708.